AD_____

Award Number: W81XWH-12-2-0123

TITLE: Rapid Field-Usable Cyanide Sensor Development for Blood and Saliva

PRINCIPAL INVESTIGATOR: Brian A. Logue

CONTRACTING ORGANIZATION: South Dakota State University, Brookings, SD 57007-0001

REPORT DATE: December 2013

TYPE OF REPORT: ANNUAL REPORT

PREPARED FOR: U.S. Army Medical Research and Materiel Command
Fort Detrick, Maryland 21702-5012

REPORT DOCUMENTATION PAGE	*Form Approved* OMB No. 0704-0188

1. REPORT DATE	2. REPORT TYPE	3. DATES COVERED *(From - To)*
December-2013	ANNUAL REPORT	26September2012-25September2013

4. TITLE AND SUBTITLE
Rapid Field-Usable Cyanide Sensor Development for Blood and Saliva

5a. CONTRACT NUMBER
W81XWH-12-2-0123

5b. GRANT NUMBER
W81XWH-12-2-0123

5c. PROGRAM ELEMENT NUMBER

6. AUTHOR(S)
Raj K. Bhandari, Brendan L. Mitchell, Randy E. Jackson, Wenhui Zhou, Robert P. Oda, and Brian A. Logue

5d. PROJECT NUMBER

5e. TASK NUMBER

5f. WORK UNIT NUMBER

7. PERFORMING ORGANIZATION NAME(S) AND ADDRESS(ES)
South Dakota State University, Brookings, SD 57007-0001

8. PERFORMING ORGANIZATION REPORT NUMBER

9. SPONSORING / MONITORING AGENCY NAME(S) AND ADDRESS(ES)

U.S. Army Medical Research and Materiel Command
Fort Detrick, Maryland 21702-5012

10. SPONSOR/MONITOR'S ACRONYM(S)

11. SPONSORING/MONITORING AGENCY REPORT NUMBER

12. DISTRIBUTION AVAILABILITY STATEMENT
Approved for Public Release; Distribution Unlimited

13. SUPPLEMENTARY NOTES

14. ABSTRACT Cyanide is a deadly poison which may be ingested or inhaled and can cause severe incapacitation or death. The diagnosis of cyanide exposure is critical to speed treatment and reduce harm. The development of a diagnostic sensor device and the identification and analysis of novel biomarkers of cyanide exposure are the major objectives of this research. Since the onset of toxic outcome from cyanide exposure is very fast, a rapid and portable sensor for the detection of cyanide exposure was developed and tested. The sensor utilized a cyanide-selective fluorescent reaction as the core chemical reaction with micro-diffusion sample preparation (previously reported). Second- and third-generation cyanide sensors were developed and the latest version is currently undergoing laboratory testing. Multiple novel markers of cyanide exposure were also identified as having potential advantages to cyanide and thiocyanate, and methods of analysis for these markers were developed or are in the process of being developed. Specifically, 2-amino-2-thiozoline-4-carboxylic acid (ATCA), alpha-ketoglutarate, and a cyanide-glutathione adduct were investigated. Toxicokinetic models were obtained through analysis of the plasma concentrations of ATCA, cyanide, and thiocyanate, analyzed from cyanide-exposed rats (previously reported), rabbits (reported in 2012), and swine, to assess the utility of ATCA as a bio-marker for cyanide exposure.

15. SUBJECT TERMS
Sensor, cyanide, thiocyanate, 2-amino-2-thiazolino-4-carboxylic acid (ATCA), toxicokinetics, biomarker, diagnostics.

16. SECURITY CLASSIFICATION OF:			17. LIMITATION OF ABSTRACT	18. NUMBER OF PAGES	19a. NAME OF RESPONSIBLE PERSON
a. REPORT	b. ABSTRACT	c. THIS PAGE			USAMRMC
U	U	U	UU	77	19b. TELEPONE NUMBER (*Include area code)*

TABLE OF CONTENTS

LIST OF FIGURES (v)

LIST OF TABLES (ix)

INTRODUCTION (1)

SECTION 1 (5)

DEVELOP A DIAGNOSTIC SENSOR THAT COMBINES RAPID AND ACCURATE DETERMINATION OF CYANIDE EXPOSURE WITH SIMPLISTIC USE AND PORTABILITY.

CHAPTER 1 (5)

DEVELOP AN EASY-TO-USE TWO-CHAMBER TYPE DIAGNOSTIC SENSOR TECHNOLOGY THAT HAS THE ABILITY TO DETERMINE CYANIDE EXPOSURE RAPIDLY AND ACCURATELY
Randy E. Jackson and Brian A. Logue

CHAPTER 2 (19)

TEST THE SENSOR DEVELOPED IN TASK 1 USING AN APPROPRIATE ANIMAL MODEL TO CONFIRM THE ABILITY OF THE SENSOR TO DIAGNOSE CYANIDE EXPOSURE.
Randy E. Jackson and Brian A. Logue

SECTION 2 (24)

EVALUATE NOVEL MARKERS OF CYANIDE EXPOSURE TO HELP DETERMINE THE MOST APPROPRIATE CYANIDE EXPOSURE MARKER

CHAPTER 3 (24)

CYANIDE TOXICOKINETICS IN A SWINE MODEL
Raj K. Bhandari and Brian A. Logue

CHAPTER 4 (28)

OPTIMIZATION AND VALIDATION OF AN ANALYTICAL METHOD TO ANALYZE, CYANIDE, THIOCYANATE AND ATCA SIMULTANEOUSLY
Raj K. Bhandari and Brian A. Logue

CHAPTER 5 (40)

DETERMINATION OF THE CYANIDE METABOLITE α-KETOGLUTARATE CYANOHYDRIN BY LIQUID CHROMATOGRAPHY TANDEM MASS-SPECTROMETRY
Brendan L. Mitchell and Brian A. Logue

CHAPTER 6 (50)

DETERMINATION OF THE CYANIDE ADDUCT OF GLUTATHIONE BY HIGH PERFORMANCE LIQUID CHROMATOGRAPHY
Wenhui Zhou, Robert P. Oda, and Brian A. Logue

CHAPTER 7 (65)

DEVELOPMENT OF AN ASSAY FOR DIMETHYL TRISULFIDE, A POTENTIAL THERAPEUTIC AGENT AGAINST CYANIDE TOXICITY
Wenhui Zhou and Brian A. Logue

LIST OF FIGURES

Figure 1.1.1-1. Schematic of the stacked configuration of the cyanide capture apparatus.

Figure 1.1.1-2. Comparison of spiked and nonspiked swine whole blood with an aqueous cyanide standard.

Figure 1.1.1-3. Optimization data for the stacked configuration of the cyanide capture apparatus using the silicone septa as a separation membrane.

Figure 1.1.1-4. Comparison of the calibration curves obtained using either a PE frit or silicone septa with tubing as a membrane. The use of 20 and 50 mL air injection volumes is also compared.

Figure 1.1.1-5. Analysis of the possible interfering agents NH_4OH (30 µM), 1 mM NaSCN and HSA (3.3 mg/mL), and 0.6 mM NaHS. Samples labeled as false negatives were spiked with 20 µM NaCN.

Figure 1.1.2-1. Configuration of the bubble-pack microdiffusion cartridge.

Figure 1.1.2-2. Bubble portion of the bubble cartridge. A) The bubble mounting pegs and B) the bubbles (modified latex balloons) attached to the bubble mounting pegs.

Figure 1.1.3-1. The cyanide sensor prototype: A) the front, left hand view of the sensor; B) the response for no exposure; and C) the flashing response for exposure.

Figure 1.2-1. Calibration curve for rabbit whole blood standards. Exposed rabbit samples (15-, 25-, and 35-min) and the cyanide-spiked blood (10 µM) QC standard are shown as overlays on the calibration curve.

Figure 2.3-1. Plasma CN^-, SCN^-, and ATCA normalized concentrations after 0.17 mg/kg/min KCN intravenous infusion to swine. Error bars are plotted as standard error of mean (SEM) (N = 11). Apnea occurred at 10 minutes, and the infusion of KCN was stopped.

Figure 2.4-1. Schematic representation of the reaction of NDA and taurine in the presence of cyanide to form an N-substituted 1-cyano [f] benzoisoindole (CBI) complex.

Figure 2.4-2. Schematic representation of the monobromobimane thiocyanate reaction to form a SCN-bimane product.

Figure 2.4-3. Overlaid chromatograms depicting the determination of cyanide, thiocyanate, and ATCA from spiked swine plasma samples. The analytes were individually spiked into plasma and the samples analyzed separately.

Figure 2.4-4. Chromatograms of 100 µM cyanide and 100 µM thiocyanate spiked into swine plasma. The chromatograms represent signal response to the MRM transitions of 298.6 → 190.7 and 248.0 → 111.0 after sample preparation and analysis for cyanide and thiocyanate, respectively. Cyanide and thiocyanate eluted from the column at approximately 6.0 and 4.0 minutes, respectively.

Figure 2.4-5. Chromatogram of 75 µM ATCA spiked into swine plasma. The chromatogram represents signal response to the MRM transition 145.0 → 67.0 after sample preparation and analysis for ATCA. ATCA eluted from the column at approximately 1.0 minute.

Figure 2.4-6. Chromatograms of potassium cyanide-exposed (1.7 mg/kg) swine plasma and non-exposed swine plasma (*lower trace*), both without internal standard. The chromatograms represent the signal response of the MRM transition 298.6 → 190.7 and 248.0 → 111.0 *m/z* transition for cyanide and thiocyanate, respectively.

Figure 2.5-1. Proposed reaction pathway for the conversion of α-Kg into α-KgCN.

Figure 2.5-2. Chromatograms of α-KgCN spiked swine plasma (upper trace) and the plasma of cyanide-exposed swine, pre-exposure (lower trace), and post-exposure (middle trace).

Figure 2.5-3. Plasma concentrations (μM) of α-KgCN, cyanide, thiocyanate, and ATCA in untreated swine over time (min). Apnea, pre-exposure and 5-min infusion sample points are designated as "time 0, -10, and -5", respectively. The plasma sampled at time zero was gathered prior to treatment, the -10 time point was obtained before infusion and the -5 time point was collected 5 min after exposure. Error bars denote SEM.

Figure 2.6-1. Reaction scheme for the condensation of cyanamide with reduced glutathione (GSH), and possible rearrangement of the initial product.

Figure 2.6-2. Reaction scheme for the addition of cyanide to oxidized glutathione (GSSG), and possible products.

Figure 2.6-3. Overlaid HPLC chromatograms of a reagent blank, the reaction mixture from GSH and cyanamide, and Fraction 8 eluted by 20% methanol in chloroform solvent from the silica column. HPLC conditions: Column: Zorbax C-18, 4.6 X 150 mm; Mobile phase: 1mM ammonium formate in water/ methanol; Flow: 1.0 mL/ min; Detection: 270 nm.

Figure 2.6-4. Overlaid HPLC chromatograms of a reagent blank, the reaction mixture from GSH and cyanamide, and Fractions 11 and 22 eluted by 50% methanol in water from the silica column. HPLC conditions: Column: Zorbax C-18, 4.6 X 150 mm; Mobile phase: ammonium formate (1 mM) in water/methanol; Flow: 1.0 mL/ min; Detection: 270 nm.

Figure 2.6-5. Overlaid mass spectra of the cyanide-spiked plasma reaction mixtures. 100 mM CN (red), 10 mM CN (green), and a plasma blank (blue). AB Sciex Q-trap 5500 Mass Spectrometer in positive ion mode with an ESI source.

Figure 2.6-6a. Possible structure for the observed m/z = 279 fragment.

Figure 2.6-6b. Possible structures for the m/z = 213 fragment.

Figure 2.7-1. Overlaid mass spectra of the DMTS-spiked NaBr solution mixtures. 0.5 mM DMTS (red), 1 mM DMTS (blue) and a NaBr blank (green). AB Sciex Q-trap 5500 Mass Spectrometer in negative ion mode with an ESI source.

Figure 2.7-2. Overlaid chromatogram of the DMTS-spiked NaBr solution mixtures. 0.5 mM DMTS (red), 1 mM DMTS (blue) and a NaBr blank (green). AB Sciex Q-trap 5500 Mass Spectrometer in negative ion mode with an ESI source.

Figure 2.7-3. Average peak area of DMTS at different incubator temperatures.

Figure 2.7-4. Average peak areas of DMTS at different syringe temperatures.

Figure 2.7-5. Overlaid chromatograms of 1 mM DMTS (red), DMTS-spiked blood (purple), blood blank (green), and a methanol blank (blue).

LIST OF TABLES

Table 2.4-1. Selected MRM transitions, optimized declustering potentials (DPs), and collision energies (CEs) for the detection of CN^-, SCN^-, and ATCA by MS-MS analysis.

Table 2.4-2. The accuracy and precision of cyanide and thiocyanate analysis from spiked swine plasma by HPLC-MS-MS.

INTRODUCTION

One of the long-term goals of the *Strategic Plan and Research Agenda for Medical Countermeasures Against Chemical Threats* (August, 2007)[1] is the development of "rapid diagnostic tests and assays to identify biological markers consistent with cyanide exposure and the level of exposure". Dr. Logue has been working to identify and study biological marker behavior and to develop rapid, portable cyanide diagnostics over the last several years.[2,3] Multiple sensor technologies have been developed by the PI to move towards the ultimate sensor technology that combines rapid and accurate determination of cyanide exposure with simplistic use. The combination of these technologies should prove to be the most rapid path towards the long-term research goal of cyanide diagnostic development. Therefore, one objective of the proposed work is to develop a diagnostic sensor that combines rapid and accurate determination of cyanide exposure with simplistic use. A diagnostic sensor will be developed from a combination of the most promising current sensor technologies for rapid cyanide diagnosis. The sensor technology will utilize the change in fluorescence from the reaction of naphthalene dialdehyde (NDA), taurine, and cyanide as the core chemical process. This chemical process has shown excellent sensitivity and selectivity for cyanide analysis in past work.

The choice of biomarker and biological matrix for diagnosing cyanide poisoning is dependent on multiple factors. While definitive determination of cyanide exposure is essential, the ability to quickly and non-invasively gather the biological matrix of interest is also desirable, especially in a mass casualty situation. Currently, cyanide exposure is

typically determined by analysis of blood for elevated cyanide concentrations, although it may not be the best matrix/biomarker combination. Therefore, multiple biomarkers will be evaluated as potential alternatives to direct analysis of cyanide by developing analytical methods for their analysis.

Technical Objectives

1. Develop a diagnostic sensor that combines rapid and accurate determination of cyanide exposure with simplistic use and portability.

2. Identify alternative biomarkers of cyanide exposure by developing analytical methods for their analysis and determining the toxicokinetics of these biomarkers.

Specific Tasks

1a) Develop an easy-to-use two-chamber type diagnostic sensor technology that has the ability to determine cyanide exposure rapidly and accurately.

Previously, the development of a simple, field-portable fluorometric sensor platform was undertaken. Although extremely promising, the analysis time for cyanide by the initial sensor was slow (5-minute analysis) compared to the onset of the symptoms of cyanide exposure. Thus, the development of the next-generation portable fluorometric cyanide diagnostic sensor will be pursued.

1b) Test the sensor developed in Task 1 using an appropriate animal model to confirm the ability of the sensor to diagnose cyanide exposure.

2) Evaluate novel markers of cyanide exposure to help determine the most appropriate cyanide exposure marker.

A rat model was used in the initial toxicokinetic experiment and may not be appropriate for this study. Therefore, a rabbit model (reported last year) and a swine model will be used to verify the toxicokinetic data. To increase the chances of finding a suitable cyanide diagnostic bio-marker, we shall also investigate the cyanide adduct of α-ketoglutarate, α-ketoglutarate cyanohydrin, and the cyanide adduct(s) of glutathione.

2a) Verify the toxicokinetics of ATCA, cyanide, and thiocyanate in an appropriate animal model post-cyanide exposure

2b) Optimize and validate an analytical method to analyze ATCA, cyanide, and thiocyanate simultaneously.

To lessen the burden of analyzing three compounds with three different methods, an analytical method to determine all three metabolites simultaneously will be developed at SDSU. This method will be utilized to determine ATCA, cyanide, and thiocyanate concentrations from the biological samples produced in Task 1, if validated prior to the toxicokinetic study.

2c) Determination of the cyanide metabolite α-ketoglutarate cyanohydrin by liquid chromatography tandem mass-spectrometry

2d) Determination of the cyanide adduct of glutathione by high performance liquid chromatography

2e) Development of an assay for dimethyl trisulfide, a potential therapeutic agent against cyanide toxicity.

REFERENCES

1. *Strategic Plan and Research Agenda for Medical Countermeasures Against Chemical Threats* (August, 2007), http://www.ninds.nih.gov/research/counterterrorism/counterACT_home.htm. Accessed 8/29/2012.2.

2. Youso, S. L.; Rockwood, G. A.; Lee, J. P.; Logue, B. A. 2010. *Anal Chim Acta* 677 24-28.

3. Logue, B. A.; Hinkens, D. M.; Baskin, S. I.; Rockwood, G. A. 2010. *Crit Rev Anal Chem* 44 122-147.

SECTION 1

DEVELOP A DIAGNOSTIC SENSOR THAT COMBINES RAPID AND ACCURATE DETERMINATION OF CYANIDE EXPOSURE WITH SIMPLISTIC USE AND PORTABILITY

CHAPTER 1

DEVELOP AN EASY-TO-USE TWO-CHAMBER TYPE DIAGNOSTIC SENSOR TECHNOLOGY THAT HAS THE ABILITY TO DETERMINE CYANIDE EXPOSURE RAPIDLY AND ACCURATELY

Randy E. Jackson and Brian A. Logue

1.1.1. Stacked Sensor Evaluation

The stacked sensor configuration (Figure 1.1.1-1) consisted of two chambers, a capture chamber and a sample chamber, separated by either of these two barrier designs: a 10 micron porous polyethylene frit or a 1.5 mm thick silicone septa with a 2 mm piece of 28 gauge stainless steel tubing (forward flow, sample to capture chamber only) through the center. The polyethylene frit and the septum with tubing were compared using a number of tests during the reporting period. When the polyethylene frit was used as the barrier, the linear range for cyanide quantification was found to be 20-100 µM with a detection limit of 5 µM. For the silicone septum with tubing, the linear range for cyanide quantification was found to be 5-100 µM with a detection limit of 1 µM.

When using the septum with tubing as the barrier between chambers, limited foaming was observed and a uniform pattern of bubbling was found, whereas the polyethylene frit produced more foaming. Studies have also shown that HCN gas adsorbs to the polyethylene frit material. Therefore, the septum with tubing performed better than the frit under all conditions tested and was determined to be the optimum configuration for future cyanide analysis with the stacked sensor configuration.

The stacked sensor was used to assess spiked and non-spiked plasma and whole blood from swine. Plasma was spiked with NaCN (10 µM) and a 100 µL aliquot was placed in to the sample chamber and acidified. The headspace was then transferred to the capture chamber using a 20 mL volume of air and fluorescent readings were measured using an Ocean Optics USB2000+ Spectrometer. The spiked plasma gave a signal of approximately 18% of an aqueous 10 µM cyanide standard. Spiked swine whole blood (20 µM NaCN) was analyzed in a similar manner. The whole blood (Figure 1.1.1-2) gave a signal of approximately 49% of the 20 µM aqueous cyanide standard. Both swine plasma and whole blood produced protein precipitation upon addition of 1 M H_2SO_4. This precipitate is mainly protein for plasma and a mixture of blood cells and protein for the blood. Precipitate may cause the observed low cyanide recoveries by occlusion of cyanide.

The stacked sensor configuration was optimized for multiple reaction conditions. The acid concentration, the sample volume, the acid injection volume and air introduction volume were optimized using 20 µM NaCN aqueous standards. The acid concentration was varied ranging from 0.25-1 M H_2SO_4 using a 400 µL injection volume and 100 µL sample volume. The sample volume was varied ranging from 10-200 µL

using a 400 µL acid injection volume of 0.5 M H_2SO_4. The acid injection volume was varied ranging from 200-500 µL using 0.5 M H_2SO_4 and a 100 µL sample volume. For all the optimization experiments, the headspace was then transferred to the capture chamber using a 20 mL volume of air and fluorescent readings were measured using an Ocean Optics USB2000+ Spectrometer. The optimization data can be seen in Figure 1.1.1-3. For aqueous solutions the optimized conditions were found to be a 0.5 M H_2SO_4 acid concentration, a 100 µL sample volume, and a 300 µL acid injection volume. The air introduction volume was varied ranging from 20-50 mL of air using the optimized reagent conditions stated above. The optimized air injection volume was found to be 50 mL of air. A comparison of the calibration curves for the polyethylene frit (20 mL air injection volume) and the silicone septa with 20 and 50 mL injection volumes can be seen in Figure 1.1.1-4. The use of the 50 mL air volume has a steeper slope for the calibration curve which createsa more sensitive sensor compared to the use of 20 mL air injection volumes, regardless of the separation membrane used.

The stacked sensor was then used to analyze compounds that could possibly interfere with the reaction of NDA, taurine and cyanide. The compounds evaluated as possible interefering agents were NH_4OH (30 µM), 1 mM NaSCN and HSA (3.3 mg/mL), and 0.6 mM NaHS. These compounds were also analyzed as the following mixtures to determine if any additive effects were a concern for these molecules: 1) equal parts of 0.55 g/mL NaHS and 30 µM NH_4OH, 2) equal parts of 1 mM NaSCN and 30 µM NH_4OH, 3) 1 mM NaSCN, Mixture 1 and HSA, 4) equal parts of 1 mM NaSCN and HSA, 5) equal parts of Mixture 1 and HSA. The intereferents were also analyzed as 20 µM NaCN spiked solutions. For all the interference samples, a 100 µL sample volume and

a 300 µL acid(0.5 M H_2SO_4) injection was used. The headspace was then transferred to the capture chamber using a 50 mL volume of air and fluorescent readings were measured using an Ocean Optics USB2000+ Spectrometer. The identification of interferents is important to assess the possibility of false positives for a particular analytical method. Figure 1.1.1-5 shows that all compounds analyzed alone produced signals comparable to the lower limit of quantification (5 µM) and that all samples containing 20 µM NaCN concentrations produced signals similar to the 20 µM NaCN standards. All mixtures analyzed could not be considered as possibly interfering because the observed signals could not be interpreted as a false positive or a false negative. This is encouraging, because researchers have noted H_2S as a potential interfering agent for other methods of cyanide analysis. For example, the EPA ion chromatography method notes H_2S (evolved when NaHS is acidified) as an interferent, masking the presence of cyanide[1] and the cobinamide-based cyanide detection method by Dasgupta also notes H_2S as an interferent[2]. For the current method, it is promising that we have not come across an interfering agent that mimics cyanide and have yet to see a false positive.

The optimized conditions for the stacked sensor configuration (Figure 1.1-1) were found to be a 1.5 mm silicone septum pierced by a 2 mm piece of 28-gauge stainless steel tubing, a 50 mL volume of air for headspace transfer, a 100 µL sample volume, and a 300 µL acid injection volume (0.5 M H_2SO_4 for aqueous samples and 1.5 M H_2SO_4 for blood samples). Also, to date there are no known interfering agents. The sensor was successfully used to diagnose cyanide exposure in rabbits using whole blood as the sample matrix (see section 1.2).

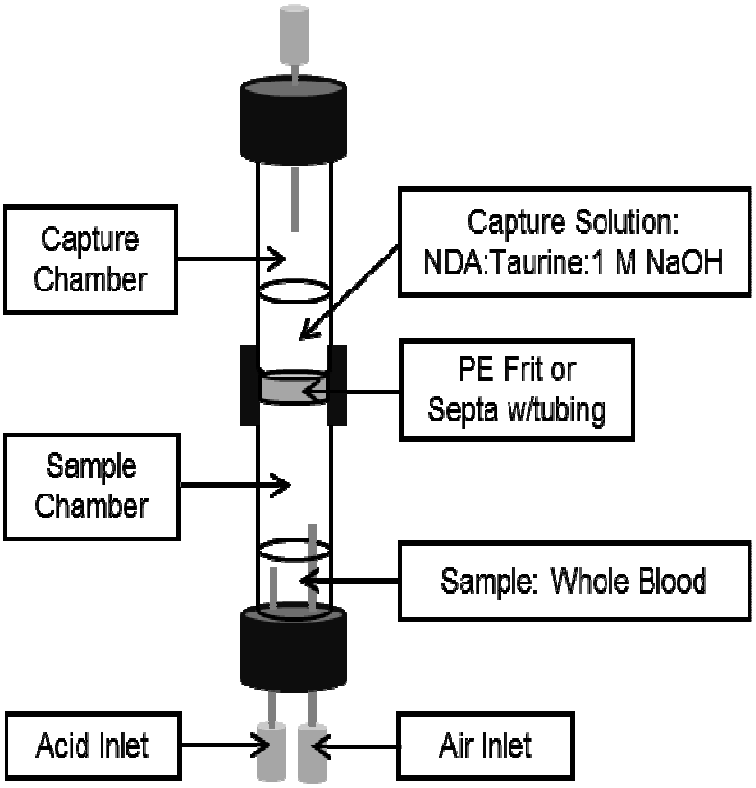

Figure 1.1.1-1. Schematic of the stacked configuration of the cyanide capture apparatus.

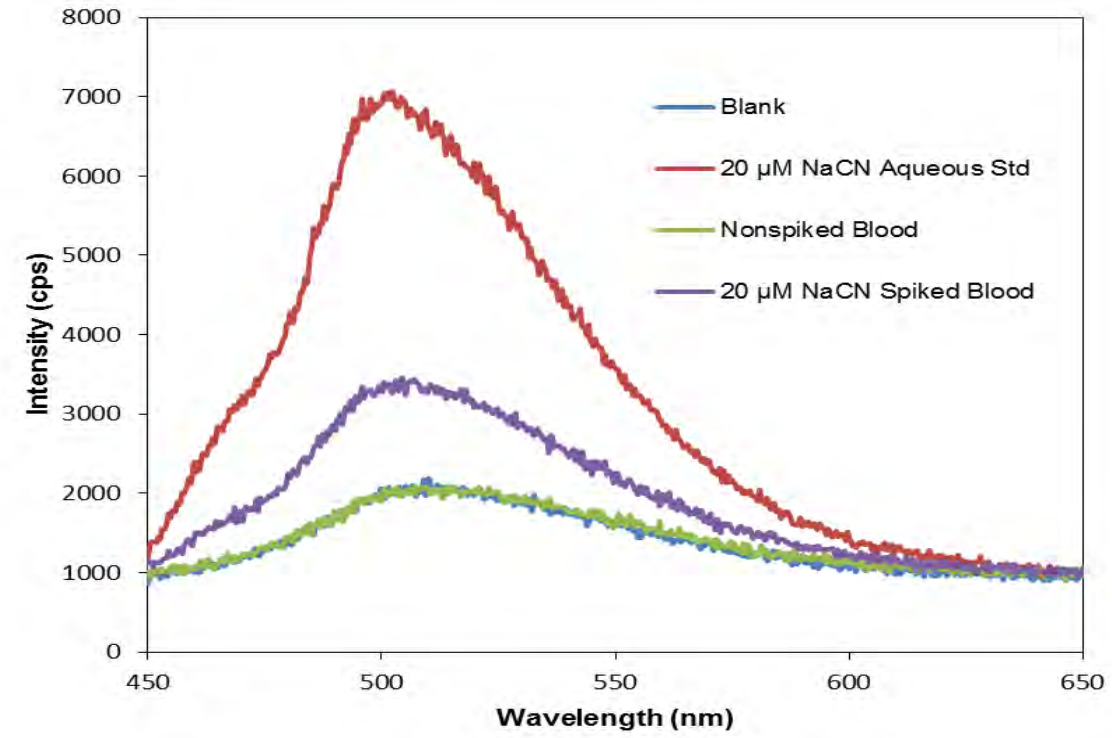

Figure 1.1.1-2. Comparison of spiked and non-spiked swine whole blood with an aqueous cyanide standard.

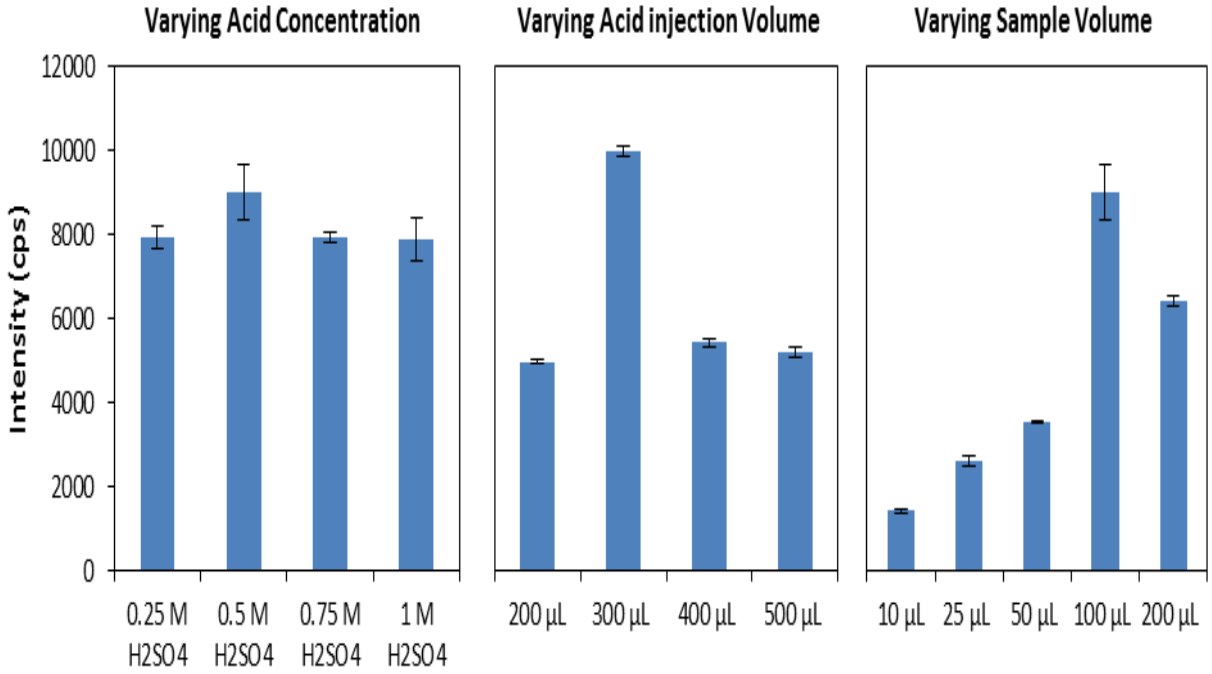

Figure 1.1.1-3. Optimization data for the stacked configuration of the cyanide capture apparatus using the silicone septa as a separation membrane.

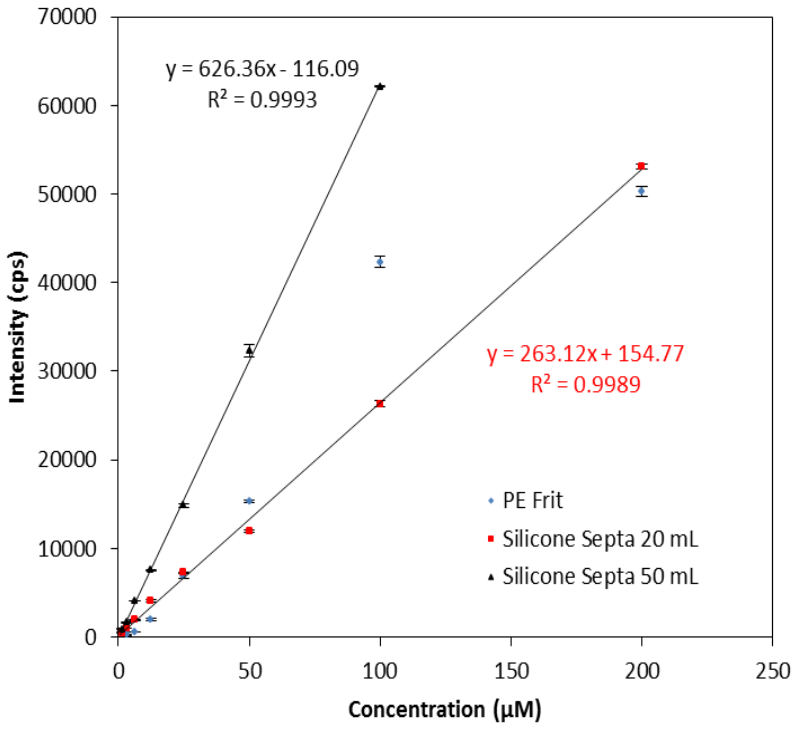

Figure 1.1.1-4. Comparison of the calibration curves obtained using either a PE frit or silicone septa with tubing as a membrane. The use of 20 and 50 mL air injection volumes is also compared.

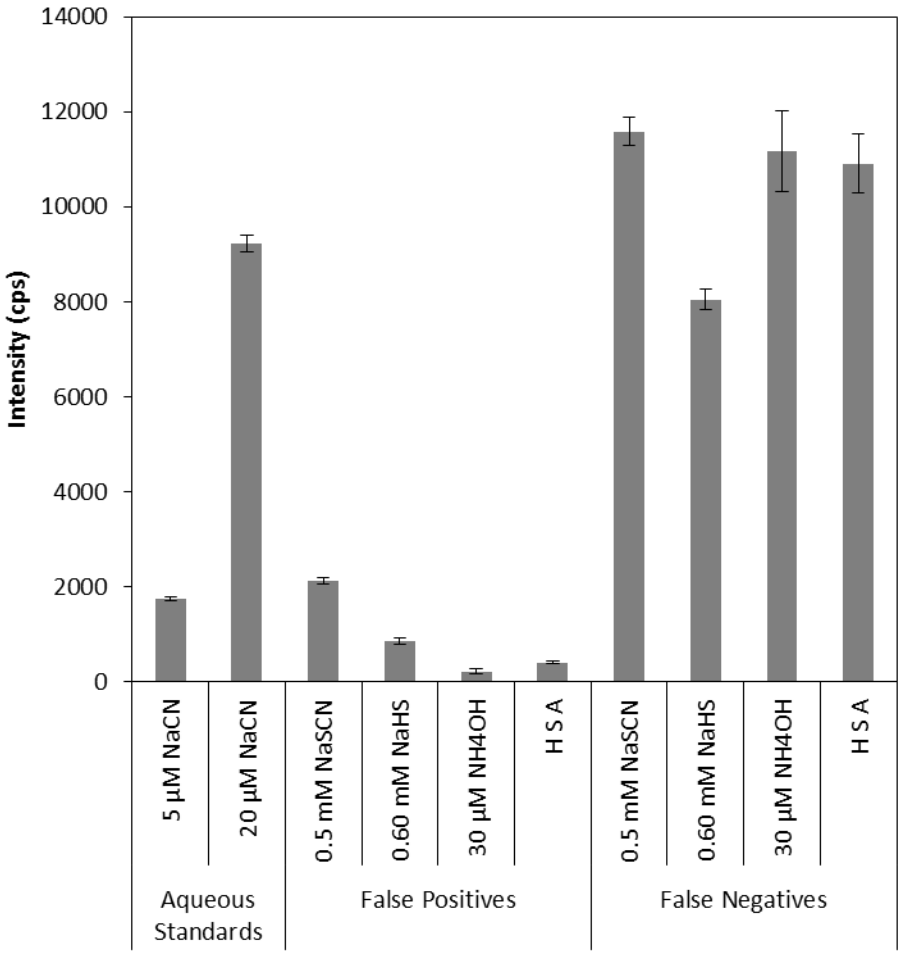

Figure 1.1.1-5. Analysis of the possible interfering agents NH_4OH (30 µM), 1 mM NaSCN and HSA (3.3 mg/mL), and 0.6 mM NaHS. Samples labeled as false negatives were spiked with 20 µM NaCN.

1.1.2. Microdiffusion Cartridge Design Evolution

A parallel track micro-diffusion design was evaluated. A "side-by-side" micro-diffusion chamber was proposed to limit the practical issues of foaming. It was found that foaming did decrease for the "side-by-side" design with the unexpected result of increased recovery compared with the stacked version. The original version of the

“side-by-side” cyanide sensor design utilized a “micro-diffusion cartridge” (not shown) with the external dimensions of 60 x 49 x 62 mm (l x w x h) and a “side-by-side” positioning of the sample and capture chambers. This cartridge used syringes attached to inlets that had channels directing specific reagents to their designated chambers. It was bulky and had design flaws that were problematic for large-scale production. A re-design of the microdiffusion cartridge gave rise to the bubble cartridge (Figure 1.1.2-1) with external dimensions of 45 x 30 x 40 mm (l x w x h) making it one-third the size of the previous version. Like the microdiffusion cartridge, the bubble cartridge utilizes a “side-by-side” positioning of the sample and capture chambers and channels to deliver the reagents to their designated chambers. However, the bubble cartridge differs because it uses bubble packets to house the reagents rather than the much larger syringes. The bubble cartridge is smaller, should increase the stability of the reagents compared with syringes, and should have higher cyanide recoveries than those of the stacked sensor.

The current microdiffusion cartridge utilizes a “bubble-pack” for reagent introduction (Figure 1.1.2-2A) with external dimensions of 45 x 30 x 40 mm (l x w x h). The bubble-pack microdiffusion cartridge utilizes side-by-side positioning of the sample and capture chambers, contains channels to deliver the reagents to their designated chambers, and uses a bubble-pack to house the reagents. Reagent storage and delivery was assessed by depressing each reagent bubble to remove air and then filling the evacuated bubble with the proper reagent. It was observed that the use of silicone to adhere the polypropylene bubbles to the side-by-side cartridge was poor. Bubble wrap was also used as a source for pre-sealed bubbles but was unsuccessful. Leakage

into the appropriate chamber (sample or capture) was a problem after pressure was applied to the reagent bubbles to release the reagent. Modified latex balloons (35 cm long with a 0.8 mm diameter) were evaluated as potential bubbles for the cartridge. The balloons were inflated sealed and allowed to sit overnight (to stretch the latex). Once the material was stretched the balloons were then cut down to 4 cm leaving the end sealed by the manufacturer intact. The balloon was slid over a 1 cm diameter test tube and then rolled to create an attached o-ring. The balloon was then stretched over the pegs (see Figure 1.1.2-2 A) to create a bubble. The complete bubble setup can be seen on Figure 1.1.2-2 B. To assess the sealing capabilities of the bubble, the balloon was depressed and then filled with 200-300 µL of water. Leakage of the filled balloon was determined and then the balloon was balloon was depressed to determine if the addition of pressure caused any leakage. The balloons were able to create a leak-free seal and could be modified to hold the correct amount of solution for the designated reagents. The latex material created the leak-free seal due to the attached o-ring and the flexibility of the material. Also, it is important to note that over time the latex became brittle and less flexible which lead to tearing. This issue will be eliminated in the manufacturing process with the use of a plastic material (i.e., the use of polyethylene) to create the bubbles.

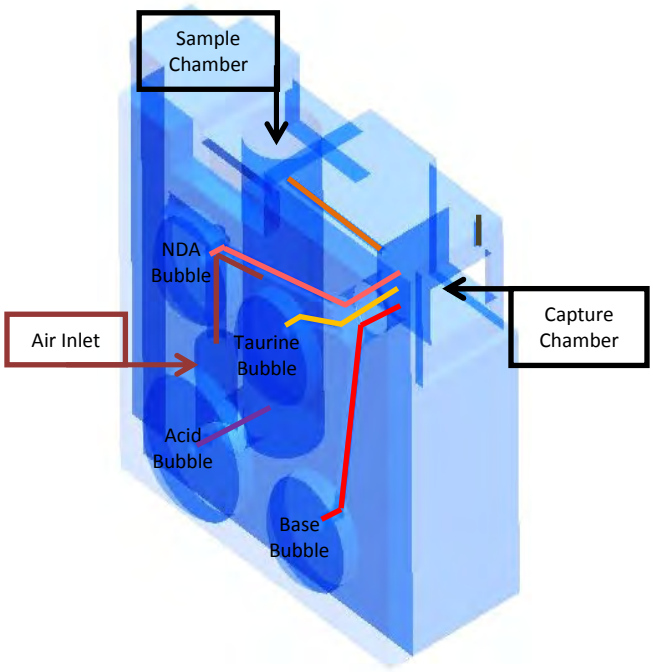

Figure 1.1.2-1. Configuration of the bubble-pack microdiffusion cartridge.

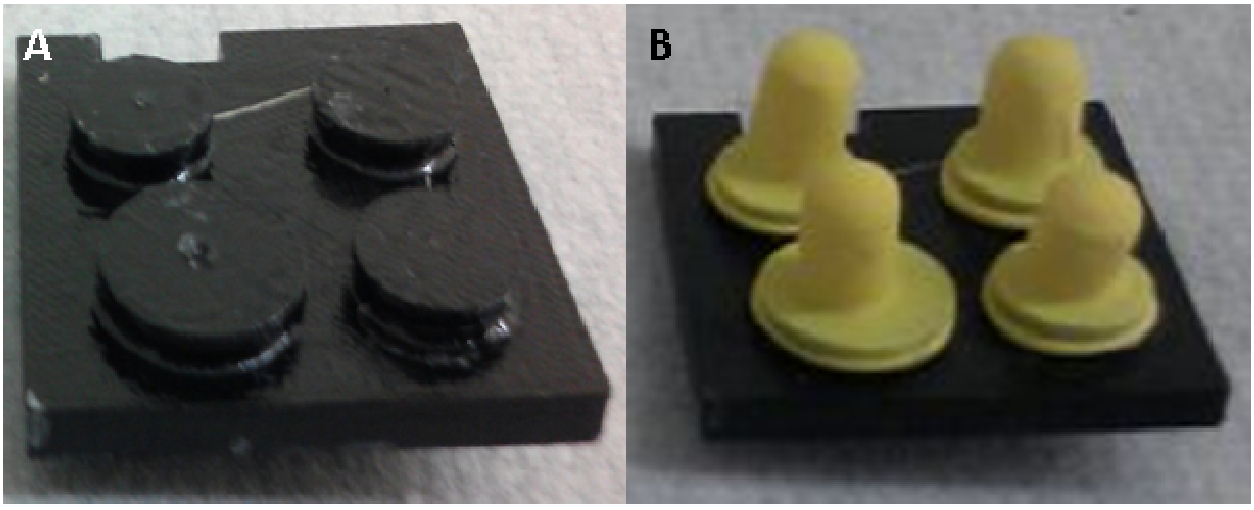

Figure 1.1.2-2. Bubble portion of the bubble cartridge. A) The bubble mounting pegs and B) the bubbles (modified latex balloons) attached to the bubble mounting pegs.

1.1.3. Sensor Circuit Design for Prototype

The addition of active transfer of HCN gas from the sample chamber to the capture chamber, and the addition of a spectrometer to lower the detection limit of the sensor made it necessary to change the circuit board design. Therefore, a detailed circuit design that incorporated a new microcontroller unit, a LCD touchscreen display, linear actuators (for air volume and reagent injection), a light-emitting diode (LED), a USB2000+ spectrometer, and all necessary electrical components (resistors, transistors, etc.) was submitted to Midwest Micro-Tek for development into a functioning custom circuit board. When completed, the circuit board was programmed so that the air volume injection, the injection of reagents, the illumination of the LED, the collection of spectral data collection, and overall sample analysis will be automated.

The sensor casing was designed and manufactured by Falcon Plastics using their fused deposition modeling FDM Printing Technology (i.e., rapid prototyping or 3D printing). The current sensor has a base for mounting all components, a cartridge and detector holder (mounted to the base and holds the microdiffusion cartridge and USB2000+ Spectrometer), and a cover (houses the display, mounts onto the base and the cartridge and detector holder). The circuitry consists of designed circuits arranged on a Microchip Explorer 16 PIC development board joined to an Electronic Assembly display development board, and a Firgelli linear actuator control board. The sensor (Figure 1.1.3-1A) was programmed and can differentiate between below threshold (display reads “No Exposure” seen in Figure 1.1.3-1B) and above threshold (display flashes “Exposure Detected” seen in Figure 1.1.3-1C) concentrations of cyanide. The circuit design, implementation, and programming were performed at Midwest Micro-Tek.

For laboratory testing, further programming is needed to create an administrator screen such that numerical data can be obtained from the sensor and analyzed. The current sensor is bulky measuring 28.5 x 19.5 x 15 cm (l x w x h). The use of bulky components such as the 50 mm linear actuator, the large development circuit board, and the USB2000+ Spectrometer makes the sensor much larger than necessary. We have found some smaller components and have designed a photodiode-based spectrometer to replace the larger component in order to miniaturize the sensor and increase instrument portability. These changes in design will simplify the circuitry and programming necessary for the sensor, as well as extend the battery life. The circuitry for the addition and removal of designated components of the current circuit design are currently being developed. In addition, the coding and communication programming for additional display screens functions, other peripheral components (i.e., linear actuator, pressure pump, etc.) and the microprocessing unit are being developed.

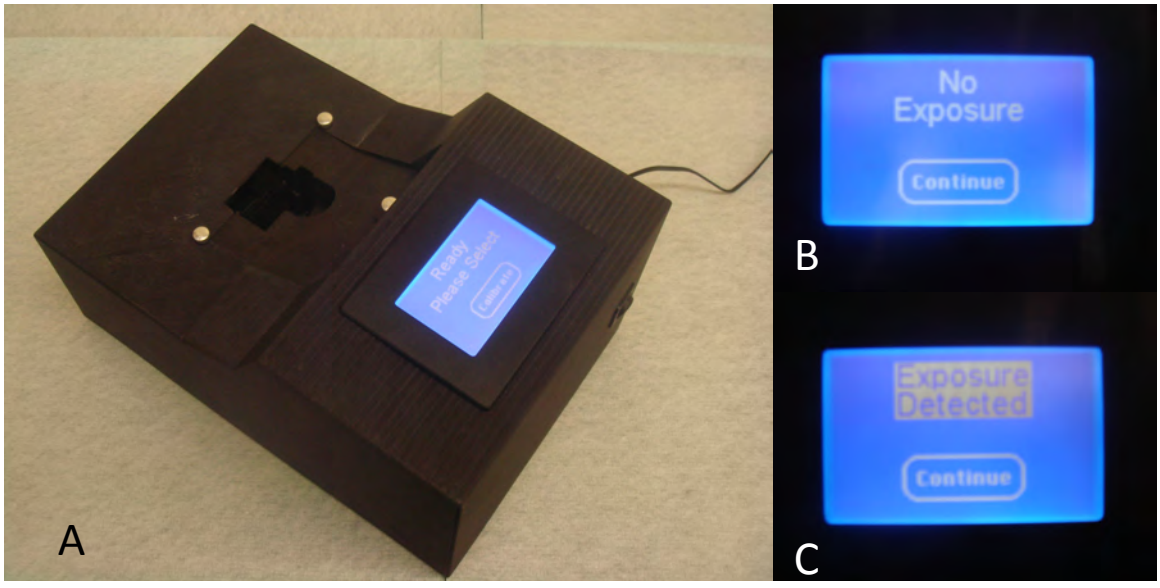

Figure 1.1.3-1. The cyanide sensor prototype: A) the front, left hand view of the sensor; B) the response for no exposure; and C) the flashing response for exposure.

REFERENCES

1. Other Test Method 29 - Sampling and Analysis for Hydrogen Cyanide Emissions from Stationary Sources. EPA, Ed., 2011.

2. Ma, J. Dasgupta, P. K. Blackledge, W. Boss, G. R. 2010. Cobinamide-Based Cyanide Analysis by Multiwavelength Spectrometry in a Liquid Core Waveguide. *Anal Chem 82*, 6244-6250.

CHAPTER 2

TEST THE SENSOR DEVELOPED IN TASK 1 USING AN APPROPRIATE ANIMAL MODEL TO CONFIRM THE ABILITY OF THE SENSOR TO DIAGNOSE CYANIDE EXPOSURE.

Randy E. Jackson and Brian A. Logue

1.2. Determination of Cyanide exposure in rabbits

Rabbit whole blood was optimized for sample volume, acid injection volume, and acid concentration using the stacked sensor. Sample volume was assessed for 50 and 100 µL, the acid injection volume ranged from 200-500 µL, and the acid concentration was assessed over the range of 0.25 to 2 M. These optimized conditions for whole blood were found to be a 100 µL sample volume and a 300 µL acid (1.5 M H_2SO_4). The acid concentration needed to evolve HCN gas from blood was more stringent than that of aqueous solutions because blood is a more complex matrix. Once the optimum conditions were determined a calibration curve was created for spiked rabbit blood standards ranging from 0.25 to 200 µM. The calibration curve can be seen in Figure 1.2-1. Fluorescent readings were measured using an Ocean Optics USB2000+ Spectrometer.

Rabbit whole blood samples were obtained from two sources: 1) non-sterile whole blood with 2.5% EDTA from young rabbits was purchased from Pel-Freeze Biologicals (Rogers, AR, USA), and 2) whole blood from cyanide-exposed male (3.5-4.5 kg), New Zealand White rabbits (*Oryctologus cuniculus*), was obtained from the University of California, Irvine. Rabbits (n = 3) were intravenously administered lethal

doses of 6.8 mM NaCN in 0.9% NaCl (1 mL/min) and blood was drawn prior to and 15, 25, and 35 minutes following the initiation of cyanide administration. The blood samples were placed in EDTA tubes to prevent coagulation. The blood samples were then frozen and shipped on ice (overnight) to South Dakota State University for analysis of cyanide. Upon receipt, the blood was stored at -80 ℃ until cyanide analysis was performed. In addition to the cyanide-exposed rabbit samples, a cyanide (10 µM) spiked blood sample was analyzed for quality control (QC) purposes and it represents the highest cyanide concentration observed in smokers [1]. Fluorescence readings were taken using an Ocean Optics USB2000+ Spectrometer.

For rabbit whole blood, the linear range was found to be 3.125-200 µM NaCN with a detection limit of 0.78 µM NaCN; the calibration curve can be seen in Figure 1.2-1. The baseline sample for the cyanide-exposed rabbit blood produced a signal that was below the lower limit of quantification (LLOQ) and could not be quantified. The 15-, 25-, and 35-minute exposed rabbit samples and the 10 µM QC standard gave calculated concentrations of 40.2 ± 8.2, 62.7 ± 15.3, 93.0 ± 11.6 µM and 9.6 µM, respectively; these data points can be seen overlaid in Figure 1.2-1. There were some discrepancies between the LODs and linear ranges of the calibration curves presented for the aqueous samples and the whole rabbit blood samples, but that was expected considering that whole blood is a more complex matrix.

When comparing blood to aqueous solutions, the non-spiked blood gave a slightly increased signal (200 -500 cps greater) than the aqueous blank at 500 nm which was expected due to endogenous levels of cyanide. Also when comparing blood and aqueous calibrations standards ranging from 3.12-100 µM, the recoveries for cyanide

based on corrected fluorescence signal ranged from 46-95%. Even with optimization, the recovery of cyanide was low (39 and 34% for 5 and 75 µM QC standards, respectively). The inefficient recovery of cyanide was likely caused by its rapid transformation to volatile HCN gas at pH values below its pKa of 9.2[2] and enzyme-catalyzed conversion to SCN^- in the presence of a sulfur donor[3,4]. Cyanide also has an affinity for hemoglobin (Hb), methemoglobin (metHb), thiols and disulfides[3,4].

Assessment of the accuracy of the stacked cyanide sensor compared to other sample preparation and analytical methods (i.e., liquid-liquid extraction, LC/MS/MS, etc.) is the next step for further validation of the sensor. Confirmation of the results obtained using the cyanide sensor technology with another analytical method would reinforce the validity of the sensor.

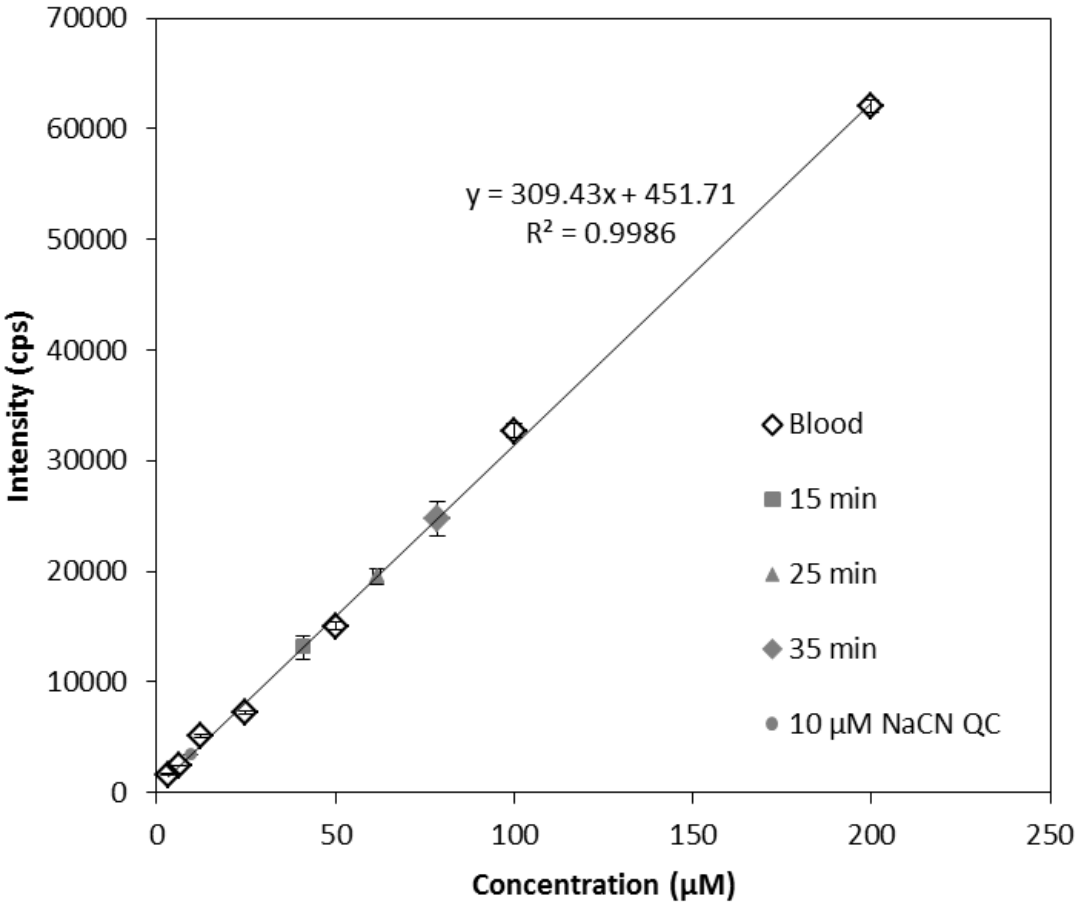

Figure 1.2-1. Calibration curve for the rabbit whole blood standards. Exposed rabbit samples (15-, 25-, and 35-min) and cyanide-spiked blood (10 µM) QC standard are shown as overlays on the calibration curve.

REFERENCES

1. Logue, B. A. Hinkens, D. M. Baskin, S. I. Rockwood, G. A. 2010. The Analysis of Cyanide and its Breakdown Products in Biological Samples. *Crit Rev Anal Chem 44,* 122-147.

2. Logue, B. A. Kirschten, N. P. Petrikovics, I. Moser, M. A. Rockwood, G. A. Baskin, S. I. 2005. Determination of the cyanide metabolite 2-aminothiazoline-4-carboxylic acid in urine and plasma by gas chromatography-mass spectrometry. *J Chromatogr B: Analyt Technol Biomed Life Sci 819*, 237-44.

3. Baskin, S.; Brewer, T.: 1997. Cyanide poisoning. In *Medical Aspects of Chemical and Biological Warfare*; Sidell, F., Takafuji, E., Franz, D., Eds.; Office of the Surgeon General, Department of the Army, United States of America: Falls Church, Virginia, pp 271-286.

4. Baskin, S. I.; Kelly, J. B.; Maliner, B. I.; Rockwood, G. A.; Zoltani, C. K.: 2008. Cyanide poisoning. In *Medical Aspects of Chemical Warfare*; Tuorinsky, S. D., Ed.; Office of the Surgeon General, Department of the Army, United States of America: Falls Church, Virginia, pp 371-410.

SECTION 2

EVALUATE NOVEL MARKERS OF CYANIDE EXPOSURE TO HELP DETERMINE THE MOST APPROPRIATE CYANIDE EXPOSURE MARKER

CHAPTER 3

CYANIDE TOXICOKINETICS IN A SWINE MODEL

Raj K. Bhandari and Brian A. Logue

A toxicokinetic study was performed to assess the behavior of markers of cyanide poisoning in a swine (45-57 kg) model[1] at Lackland AFB, TX. Pigs were sedated, endotracheally intubated, and maintained under anesthesia with inhaled isoflurane. Swine were infused intravenously with 0.17 mg/kg/min potassium cyanide (KCN) until apnea occurred. One minute after apnea, an antidote was administered intravenous or intraosseously over 2 minutes. The animals were then observed for an additional 60 minutes. Arterial blood (20 mL) sampling was performed at baseline (time "zero"), 5 minutes into cyanide infusion, at apnea, and every 2 minutes for the first 10 minutes after apnea, and then every 10 minutes until 60 minutes post-apnea. Four milliliters of blood were placed in EDTA tube and centrifuged to separate the plasma. The plasma samples (500 µL) were then frozen and shipped on ice to SDSU for analysis of CN^-, SCN^-, and ATCA.

The plasma samples from swine were simultaneously analyzed for CN and SCN^- by chemical-ionization (CI) GC-MS after chemical modification based on a method

previously reported[2] . Briefly, plasma samples (100 µL) were added to 2 mL micro-centrifuge vials. Internal standards (100 µL) of $Na^{13}C^{15}N$ (200 µM) and $NaS^{13}C^{15}N$ (100 µM) were added to the sample vials along with TBAS (800 µL of 10 mM TBAS in a saturated solution of sodium tetraborate decahydrate, pH 9.5) and PFB-Br (500 µL of a 20 mM solution in ethyl acetate) and vortexed for 2 minutes. Samples were then heated at 70 ºC for 1 hour, and centrifuged for 4 minutes at 10,000 rpm (9,300 x g) to separate the organic and aqueous layers. The organic layer (200 µL) was collected and analyzed using CI-GC-MS. The concentrations for both CN and SCN^- were well above the detection limit of the analytical method (approximately 1 µM for CN and 50 nM for SCN^-) for all samples analyzed.

Swine plasma samples (50 µL) were analyzed for ATCA according to a slightly modified procedure previously reported[3]. Briefly, plasma samples (80 µL), internal standard (ATCA-d_2 ; 120 µL of 100 ng/mL), and 300 µL of 1% HCl in acetone were added to a 2 mL micro-centrifuge vial, vortexed for 2 minutes and centrifuged for 4 minutes (room temperature) at 10,000 rpm (9,300 x g). The supernatant was transferred to a clean micro-centrifuge tube, 1.0 mL of 0.1 M HCl was added, and the sample was aspirated through a prepared mixed-mode cation-exchange solid phase extraction column (1 mL). The ATCA was eluted from the column into a 2 mL micro-centrifuge tube using 1 mL of a water:methanol:ammonium hydroxide solution (25:50:25, by volume). Hydrochloric acid (200 µL of 0.1 M) was added to the micro-centrifuge tube to decrease the pH of the sample (pH < 11) and the sample was dried. The dried samples were reacted with 200 µL of 30% MSTFA in hexane for 60 min at 50 ºC in capped centrifuge tubes. The samples were then analyzed using electron-

ionization GC-MS. The concentrations for ATCA were well above the detection limit of the analytical method (approximately 170 nM) for each plasma sample tested.

Figure 2.3-1 shows the normalized CN^-, SCN^-, and ATCA concentrations from swine (N = 11) during and after infusion with KCN. Plasma CN^- and ATCA concentrations reached a maximum at apnea (CN^-: 30.18 µM and ATCA: 4.73 µM) and then declined. The concentrations of each metabolite normalized to the baseline are very similar except for SCN^-. Thiocyanate concentrations rose to a maximum at apnea (≈10 minutes) and fell to a minimum (≈5 minutes post-apnea) and then continued to rise for the duration of the experiment (70 min). The concentrations of CN^-, SCN^-, and ATCA were measurable throughout the study.

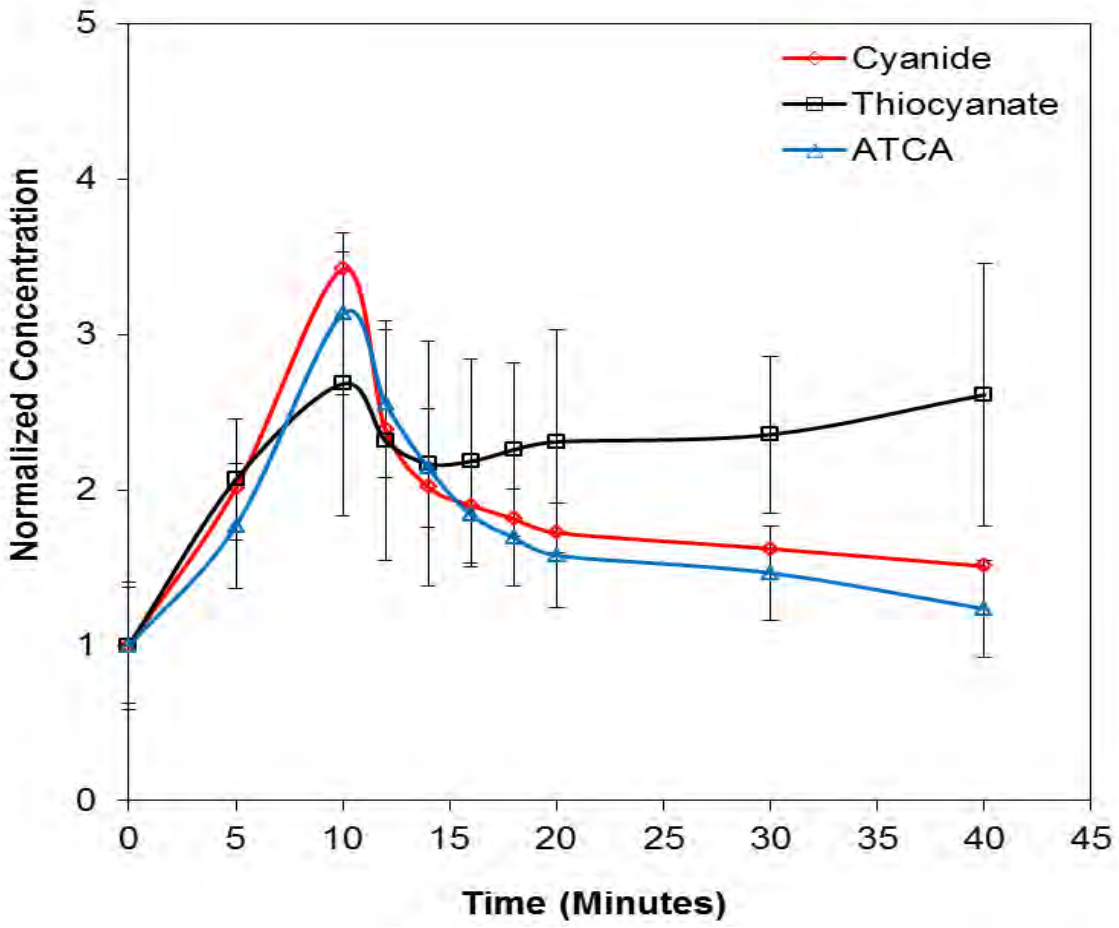

Figure 2.3-1. Plasma CN^-, SCN^-, and ATCA normalized concentrations after 0.17 mg/kg/min KCN intravenous infusion to swine. Error bars are plotted as standard error of mean (SEM) (N = 11). Apnea occurred at 10 minutes, and the infusion of KCN was stopped.

This project was completed and a manuscript detailing the investigation is in preparation for submission to *Toxicology Letters*[4].

REFERENCES

1. Bebarta, V. S.; Tanen, D. A.; Lairet, J.; Dixon, P. S.; Valtier, S.; Bush, A., 2010. Hydroxocobalamin and sodium thiosulfate versus sodium nitrite and sodium thiosulfate

in the treatment of acute cyanide toxicity in a swine (Sus scrofa) model. *Annals of Emergency Medicine* 55 (4), 345-51.

2. Bhandari, R.K., Oda, R.P., Youso, S.L., Petrikovics, I., Bebarta, V.S., Rockwood, G.A., Logue, B.A., 2012. Simultaneous determination of cyanide and thiocyanate in plasma by chemical ionization gas chromatography mass-spectrometry (CI-GC-MS). *Analytical and Bioanalytical Chemistry* 404, 2287-2294.

3. Logue, B.A., Kirschten, N.P., Petrikovics, I., Moser, M.A., Rockwood, G.A., Baskin, S.I., 2005. Determination of the cyanide metabolite 2-aminothiazoline-4-carboxylic acid in urine and plasma by gas chromatography-mass spectrometry. *J Chromatogr B: Analyt Technol Biomed Life* 819, 237-244.

4. Bhandari, R. K., Oda, R. P., Petrikovics, I., Thompson, D., Mohan, S. B., Brenner, M., Rockwood, G. A., Logue, B. A. Cyanide Toxicokinetics: The Behavior of Cyanide, Thiocyanate and 2-amino-2-thiazoline-4-carboxylic Acid (ATCA) following Cyanide Exposure (*Manuscript in preparation*).

CHAPTER 4

OPTIMIZE AND VALIDATE AN ANALYTICAL METHOD TO ANALYZE ATCA, CYANIDE, AND THIOCYANATE SIMULTANEOUSLY

Raj K. Bhandari and Brian A. Logue

To lessen the burden of analyzing three compounds with three different methods, an analytical method to determine all three metabolites simultaneously will be developed at SDSU. This method will be utilized to determine ATCA, cyanide, and thiocyanate concentrations from the biological samples produced in Task 1, if validated prior to the toxicokinetic study.

2.4. Simultaneous Assay for CN, SCN, and ATCA

The simultaneous determination of CN^-, SCN^-, and ATCA would greatly simplify the analysis of the three compounds within a single sample by reducing sample consumption, minimizing reagent cost, and enabling a more rapid analysis. Cyanide was derivatized with a mixture of naphthalene-2,3-dicarboxaldehyde (NDA, 4 mM in methanol) and taurine (50 mM in water)[1](Figure 2.4-1), thiocyanate was derivatized with monobromobimane[2] (4 mM in pH 8.0 borate buffer) (Figure 2.4-2) and ATCA was analyzed underivatized. The separation of cyanide and its metabolites were performed by a gradient of 90% 5 mM aqueous ammonium formate (as mobile phase A) and 90% 5 mM ammonium formate in methanol (as mobile phase B) using a Phenomenex Synergi 4µ Fusion-RP 80 Å column. Detection was accomplished with an AB Sciex Q-Trap 5500 mass analyzer with an ion-spray interface, operated in the negative ionization mode. Preliminary infusion studies were conducted on cyanide, thiocyanate, and ATCA to identify MRM transitions.

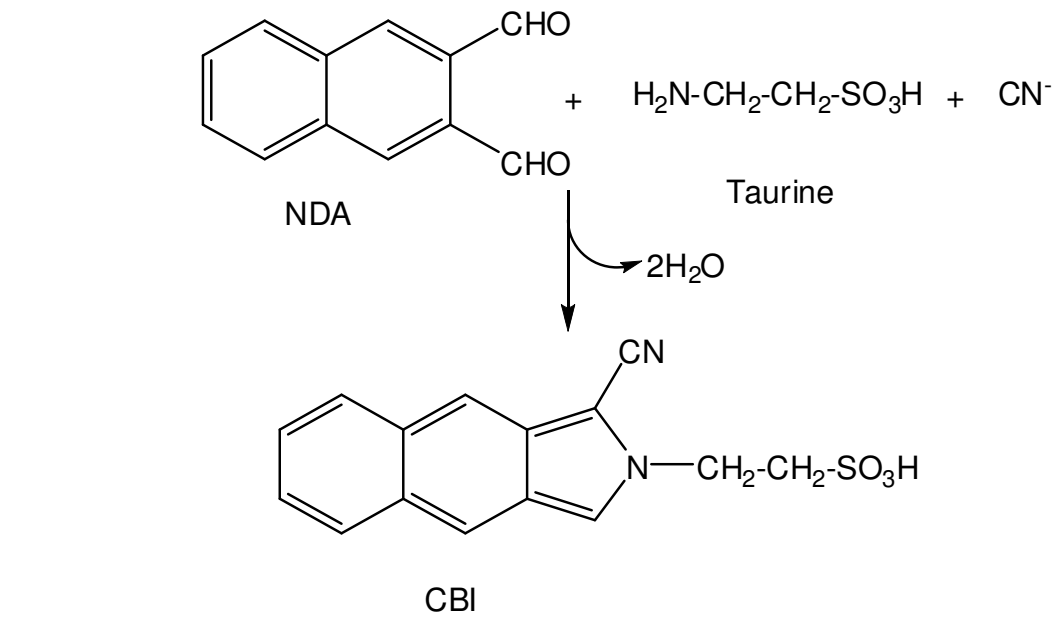

Figure 2.4-1. Schematic representation of the reaction of NDA and taurine in the presence of cyanide to form an N-substituted 1-cyano [f] benzoisoindole (CBI) complex.

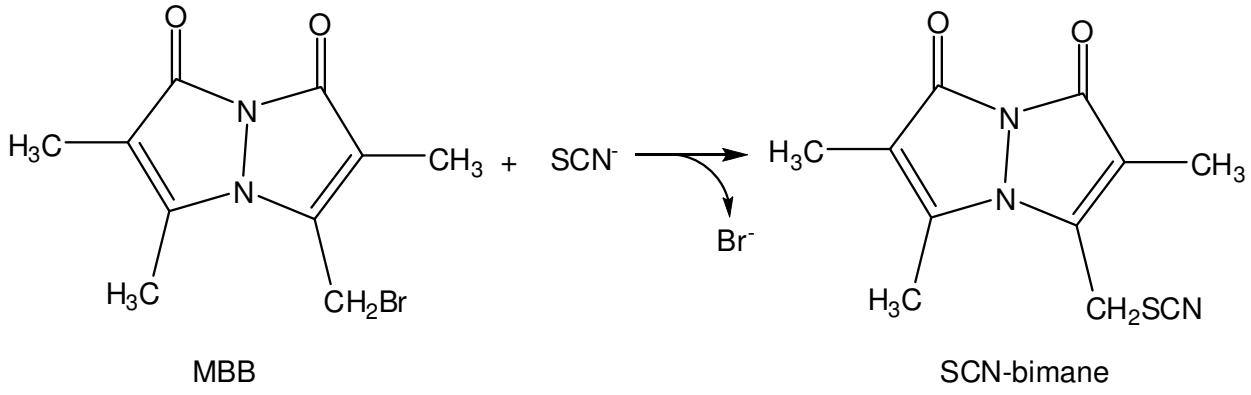

Figure 2.4-2. Schematic representation of the monobromobimane thiocyanate reaction to form a SCN-bimane product.

Detection was accomplished with an AB Sciex Q-Trap 5500 mass analyzer with an electrospray interface, operated in the negative ionization mode. Nitrogen (50 psi) was used as the curtain gas. The ion source was operated at -4500 V and a temperature of 750 ℃ with a flow rate of 90.0 psi for both the nebulizer (GS1) and heater (GS2) gasses. The collision cell was operated with an entrance potential of -10.0 V and a collision potential of -11.0 V at a medium collision gas (N_2) flow rate. CN^-, SCN^- and ATCA were analyzed by multiple reaction monitoring (MRM) with the parameters outlined in Table 2.4-1.

Table 2.4-1. Selected MRM transitions, optimized declustering potentials (DPs), and collision energies (CEs) for the detection of CN^-, SCN^- and ATCA by MS-MS analysis.

Compound	Q1 Mass (m/z)	Q3 Mass (m/z)	Time (msec)	DP (volts)	CE (volts)
CN- (quantitation)	298.6	190.7	100	-70.0	-25.0
CN- (identification)	298.5	80.9	100	-70.0	-25.0
$^{13}C^{15}N^-$ (quantitation)	300.6	192.7	100	-70.0	-25.0
$^{13}C^{15}N^-$ (identification)	300.6	80.8	100	-70.0	-25.0
SCN^- (quantitation)	248.0	111.0	100	-185.0	-19.0
SCN^- (identification)	248.0	124.1	100	-185.0	-19.0
$S^{13}C^{15}N^-$ (quantitation)	250.0	111.0	100	-185.0	-19.0
$S^{13}C^{15}N^-$ (identification)	250.0	126.1	100	-185.0	-19.0
ATCA (quantitation)	145.0	67.0	100	-110.0	-13.0

ATCA (identification)	145.0	57.9	100	-110.0	-13.0
ATCA-d_2 (quantitation)	147.0	69.0	100	-110.0	-13.0
ATCA-d_2 (identification)	147.0	57.9	100	-110.0	-13.0

These transitions were then used for analysis via UHPLC-MS-MS. All the three analytes were successfully identified in spiked swine plasma (Figure 2.4-3). As seen in Figure 2.4-3, tailing is observed for ATCA, which is most likely due to the interaction of the highly polar ATCA molecule with residual silanols on the column and will be addressed in future studies.

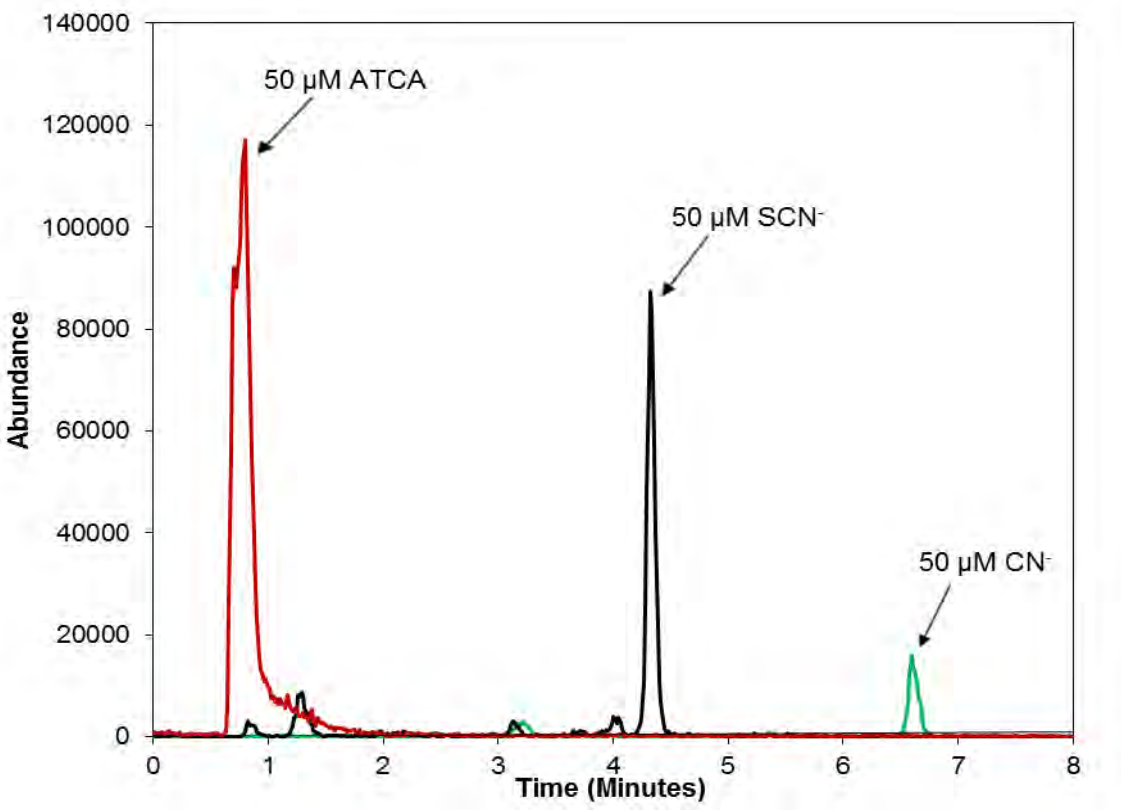

Figure 2.4-3. Overlaid chromatograms depicting the determination of cyanide, thiocyanate, and ATCA from spiked swine plasma samples. The analytes were individually spiked into plasma and the samples analyzed separately.

Figure 2.4-4 shows the chromatograms of simultaneous analysis of derivatized cyanide and thiocyanate in spiked swine plasma and Figure 2.4-5 shows the chromatogram of underivatized ATCA. When underivatized ATCA was added to the spiked CN^- and SCN^- samples, the signal of ATCA vanished, which could be due to ATCA reacting with other components in the spiked plasma samples referred to as 'matrix effect'. Once the issues with ATCA are resolved, the method will be subsequently validated and figures of merit (e.g., limit of detection, precision, accuracy, linear range) will be established.

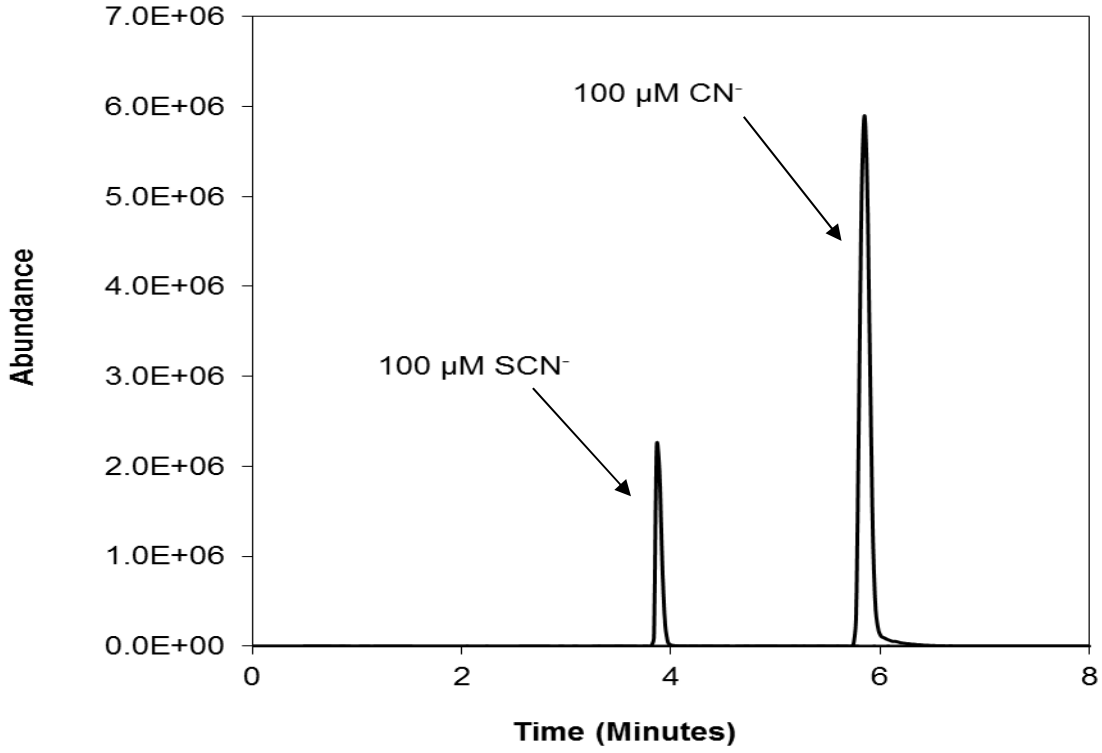

Figure 2.4-4. Chromatograms of 100 µM cyanide and thiocyanate spiked into swine plasma. The chromatograms represent signal response to the MRM transitions of 298.6 → 190.7 and 248.0 → 111.0 after sample preparation and analysis for cyanide and thiocyanate, respectively. Cyanide and thiocyanate eluted from the column at approximately 6.0 and 4.0 minutes, respectively.

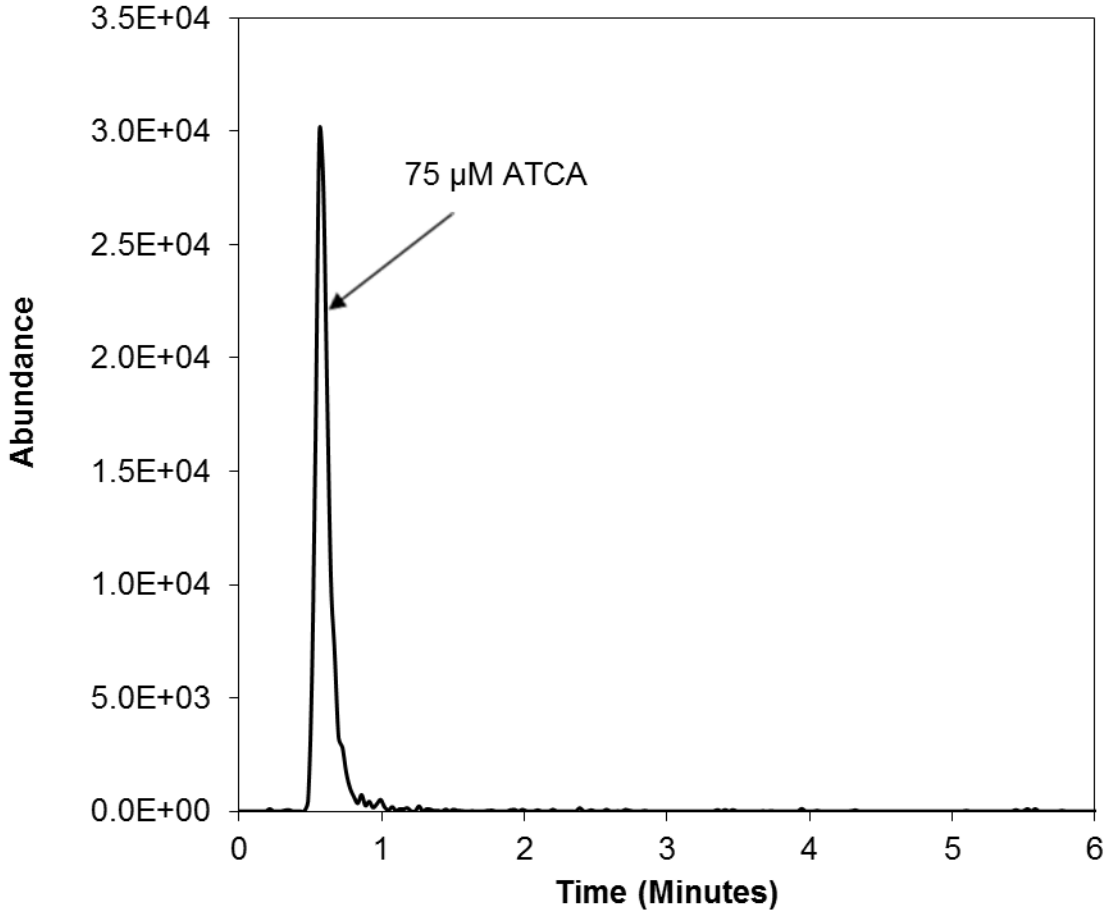

Figure 2.4-5. Chromatogram of 75 µM ATCA spiked into swine plasma. The chromatogram represents signal response to the MRM transition 145.0 → 67.0 after sample preparation and analysis for ATCA. ATCA eluted from the column at approximately 1.0 minute.

Due to the difficulties in analyzing ATCA in conjunction with CN^- and SCN^-, the focus of this project was altered to develop an analytical method to simultaneously determine cyanide and thiocyanate using a high-performance liquid chromatography tandem mass-spectrometry (HPLC-MS-MS). Thus, an analytical procedure for the simultaneous determination of cyanide and thiocyanate was developed and validated in

swine plasma generally according to Food and Drug Administration (FDA) guideline[3]. The sample preparation was simple and quick, with cyanide and thiocyanate simultaneously analyzed by high-performance liquid chromatography mass spectrometry in negative ionization mode. Isotopically labeled internal standards, $Na^{13}C^{15}N$ and $NaS^{13}C^{15}N$, were mixed with swine plasma (spiked and non-spiked). Proteins were precipitated with acetone, the samples were centrifuged, and the supernatant was removed and dried. The dried samples were reconstituted in 10 mM ammonium formate. Cyanide was reacted with naphthalene-2,3-dicarboxaldehyde (NDA) and taurine to form N-substituted 1-cyano [f] benzoisoindole (CBI)[1] (Figure 2.4-1), while thiocyanate was reacted with monobromobimane[2] to form an SCN-bimane product (Figure 2.4-2). The method produced a dynamic range of 0.1-50 and 0.2-50 µM for cyanide and thiocyanate, respectively, with limits of detection of 10 nM for cyanide and 50 nM for thiocyanate. For all the quality control standards analyzed, the precision, as measured by %RSD, was below 8%, and the accuracy was within ±10% of the nominal concentration (Table 2.4-2).

Table 2.4-2. The accuracy and precision of cyanide and thiocyanate analysis from spiked swine plasma by HPLC-MS-MS.

		Intraassay		Interassay	
Analyte	**Concentration (µM)**	**Accuracy (%)[a]**	**Precision (%RSD)[a]**	**Accuracy (%)[b]**	**Precision (%RSD)[b]**
Cyanide	0.3	92.5	1.1	92.8	1.5
	3	91.6	7.3	90.6	5.4
	15	92.7	2.2	95.8	4.1
Thiocyanate	0.7	95.6	4.2	94.7	6.8
	4	94.1	3.4	95.6	3.4

	15	98.1	5.6	97.5	3.9

[a]QC method validation (N = 5) for day 3.

[b]Mean of three different days of QC method validation (N = 15).

Following validation, the analytical procedure successfully detected cyanide and thiocyanate simultaneously from cyanide-exposed swine plasma. (Figure 2.4-6). It should be noted that in the blank sample endogenous levels of both cyanide and thiocyanate could be detected and quantified. Basal concentrations of CN and SCN^- were determined to be 3.58 and 4.35 µM, respectively.

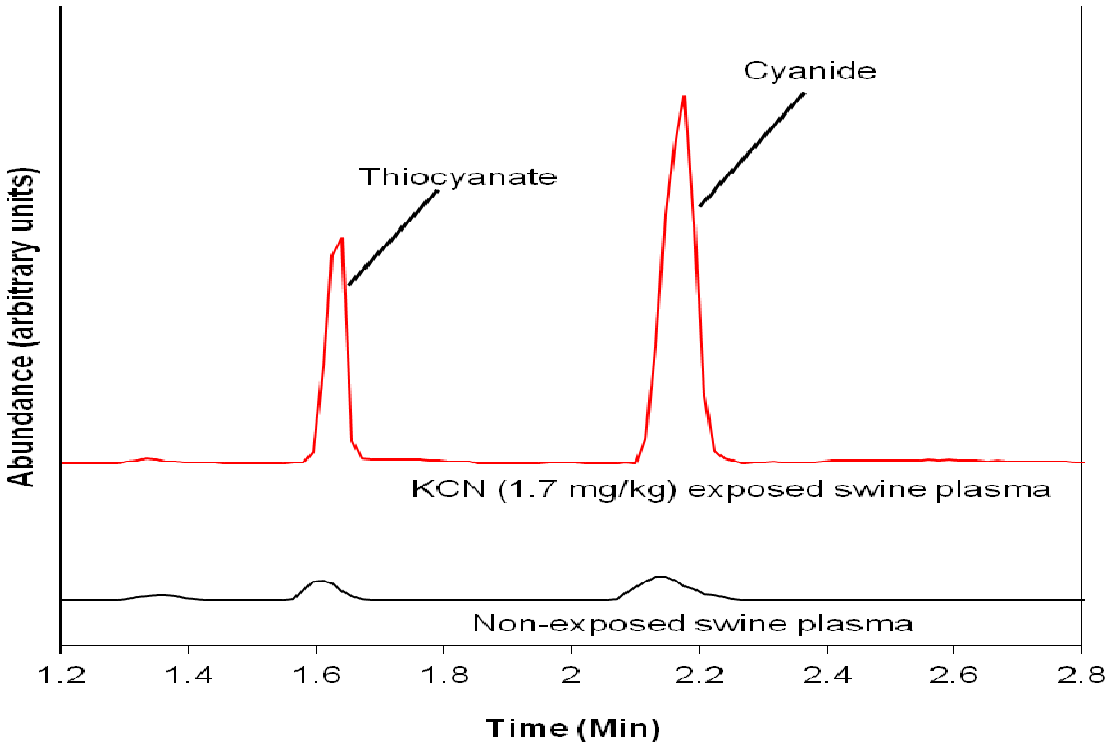

Figure 2.4-6. Chromatograms of potassium cyanide-exposed (1.7 mg/kg) swine plasma and non-exposed swine plasma (*lower trace*), both without internal standard. The chromatograms represent the signal response of the MRM transition 298.6 → 190.7 and 248.0 → 111.0 *m/z* transition for cyanide and thiocyanate, respectively.

Overall, the sample preparation and analysis was rapid and simple. The duration of sample preparation was approximately 40 minutes, with the chromatographic analysis lasting approximately 8 minutes (including equilibrium for the following sample). Using conservative estimates, approximately 170 parallel samples could be processed and analyzed within a 24-hour period.

This project was completed and a manuscript detailing the method has been submitted for publication to *Analytical and Bioanalytical Chemistry* journal[4].

REFERENCES

1. Sano, A., Takezawa, M., and Takitani, S., 1989. Spectrofluorometric determination of cyanide in blood and urine with naphthalene-2,3-dialdehyde and taurine. *Analyt Chim Acta* 225, 351-358.

2. Kosower, N. S. and Kosower, E. M., 1987**.** Thiol Llabeling with bromobimanes, *Meth. Enzymol* 143, 76-84.

3. *Guidance for Industry Bioanalytical Method Validation* 2001 U.S. Department of Health and Human Services, Food and Drug Administration Center for Drug Evaluation and Research (CDER), Center for Veterinary Medicine (CVM).

4. Bhandari, R. K., Manandhar, E., Oda, R. P., Rockwood, G. A., and Logue, B. A. 2013. Simultaneous high-performance liquid chromatography-tandem mass

spectrometry (HPLC-MS-MS) analysis of cyanide and thiocyanate from plasma. (*Manuscript in preparation*).

CHAPTER 5

DETERMINATION OF THE CYANIDE METABOLITE A-KETOGLUTARATE CYANOHYDRIN BY LIQUID CHROMATOGRAPHY TANDEM MASS-SPECTROMETRY

Brendan L. Mitchell and Brian A. Logue

INTRODUCTION

Cyanide exposure can occur in a variety of ways, including accidental, suicidal, or homicidal. General population exposure can occur through smoke inhalation from cigarettes or fires, consuming cyanogenic glycosides found in foods, and working in cyanogenic glycoside producing facilities[1]. Furthermore, cyanide exposure can also occur by the use of cyanide as a chemical warfare agent[2]. Because humans can be exposed to cyanide according to the routes outlined above, detection of cyanide is important to confirm exposure and administer treatment in a timely fashion. The direct analysis of cyanide to confirm exposure has various limitations, due to cyanide's volatility, reactivity, and short half-life in biological fluids, which make it difficult to detect cyanide[3-5]. Limitations associated with the direct analysis of cyanide have led to the development of biomarker analysis for indirect determination of cyanide exposure.

The focus of this project is on the development of an analytical method to determine the presence of cyanide exposure in biological fluids by detection of the

cyanide metabolite, α-ketoglutarate cyanohydrin (α-KgCN). Cyanide (HCN or CN-) is a reactive nucleophile known to interact with carbonyl compounds to form cyanohydrins[6]. In biological systems, cyanide is converted to α-ketoglutarate cyanohydrin (α-KgCN) through an equilibrium reaction with α-ketoglutarate (α-Kg) (Figure 2.5-1). Because α-Kg in the plasma[7] reacts with CN^-, the ability to determine concentrations of α-KgCN may allow for verification of cyanide exposure. Therefore, an analytical method for determining α-KgCN was pursued. Once developed, the method should be able to determine the amount of CN- that is being converted into α-KgCN and may also be beneficial in aiding therapeutic studies on α-Kg as a drug treatment for CN- poisoning.

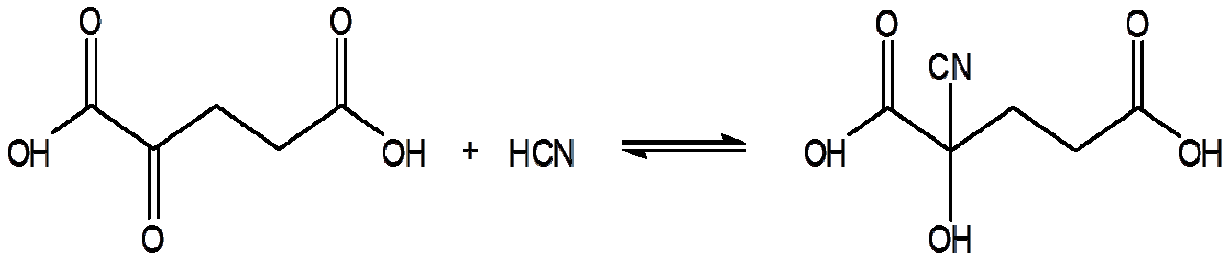

α-Kg α-KgCN

Figure 2.5-1. Proposed reaction pathway for the conversion of α-Kg into α-KgCN.

EXPERIMENTAL

Reagents and Materials

All reagents were at least HPLC grade. Sodium cyanide (NaCN) and all solvents were purchased from Fisher Scientific (Fair Lawn, NJ, USA). α-ketoglutaric acid (α-Kg)

and α-ketoglutaric acid-d_6 (α-Kg-d_6) were purchased from Sigma-Aldrich (St. Louis, MO, USA). LC/MS grade formic acid was purchased from Thermo Scientific (Rockford, IL, USA). Swine (*Sus scrofa*) plasma (non-sterile with sodium citrate anti-coagulant) was prepared from whole blood received from the Department of Animal Science at South Dakota State University (Brookings, SD, USA).

Synthesis of α-KgCN and α-KgCN-d_4

α-KgCN was synthesized by reacting equimolar equivalents of NaCN with α-Kg in water at room temperature for 30 minutes. It should be noted that α-Kg was added first and then NaCN was added to the resulting solution. After 30 minutes, the resulting solution was filtered and solvent was removed by rotary evaporation to afford a white, sticky product. Characterization was achieved by ^{13}C NMR, along with ESI-MS operated in negative polarity mode. ^{13}C NMR (CD_3OD, 400 MHz): δ 178, 120, 70. ESI(-)-MS: *m/z* 172.0, 144.7, 101.0, 44.8. An isotopically-labeled internal standard, α-KgCN-d_4 was synthesized and characterized similarly as described above for α-KgCN, with α-Kg-d_6 replacing α-Kg to afford a white solid. ^{13}C NMR (CD_3OD, 400 MHz): δ 178, 172, 122, 73. ESI(-)-MS: *m/z* 176.1, 149.1, 105.1, 44.8.

Stability Studies of α-KgCN

The stability of α-KgCN in swine plasma was evaluated on the bench-top and in the autosampler over 24 h. Prepared samples of α-KgCN exhibited excellent stability in the autosampler with no more than 15% deviation from the control. Furthermore, freeze-thaw experiments showed that α-KgCN was stable in swine plasma at -80 ºC

over the 3 cycles tested. Conversely, the bench-top stability of α-KgCN was poor with α-KgCN concentrations falling significantly below 85% of the control within 2 h, showing that α-KgCN is quickly eliminated from swine plasma at room temperature. The α-KgCN was stable at both low and high QC concentrations for 30 days at -80 °C, for 1 day at -20 °C, and was quickly eliminated at 4 °C. The results of the long-term study suggest that α-KgCN-spiked swine plasma samples should be stored at -80 °C when possible.

Recovery experiments were conducted in order to determine the ability of the sample preparation protocol to extract α-KgCN from swine plasma. The recovery of α-KgCN from swine plasma at low, medium, and high QC concentrations was 14%, 22%, and 27%, respectively. Acidification of the swine plasma before spiking in α-KgCN, did not significantly increase the recovery (25%, 23%, and 30% for low, medium and high QC samples, respectively). Heating the swine plasma before spiking in α-KgCN, decreased the recovery (7%, 4%, and 4% for low, medium, and high QC samples, respectively). Because enyzme activity should at least be reduced when acidifying or heating the plasma, the consistently low recovery, is most likely due to facile chemical processes, such as protein binding, ATCA formation, or evaporation of HCN.

The described method was applied to the analysis of α-KgCN in swine plasma samples obtained from cyanide-exposed pigs. The peak for α-KgCN was observed around 1.6 min (Figure 2.5-2). The absence of co-eluting peaks in the pre-exposed swine sample indicates that the analysis is selective for α-KgCN.

Overall, the results indicate that the analytical method presented here can be used to quickly and easily analyze α-KgCN in the plasma of cyanide-exposed swine.

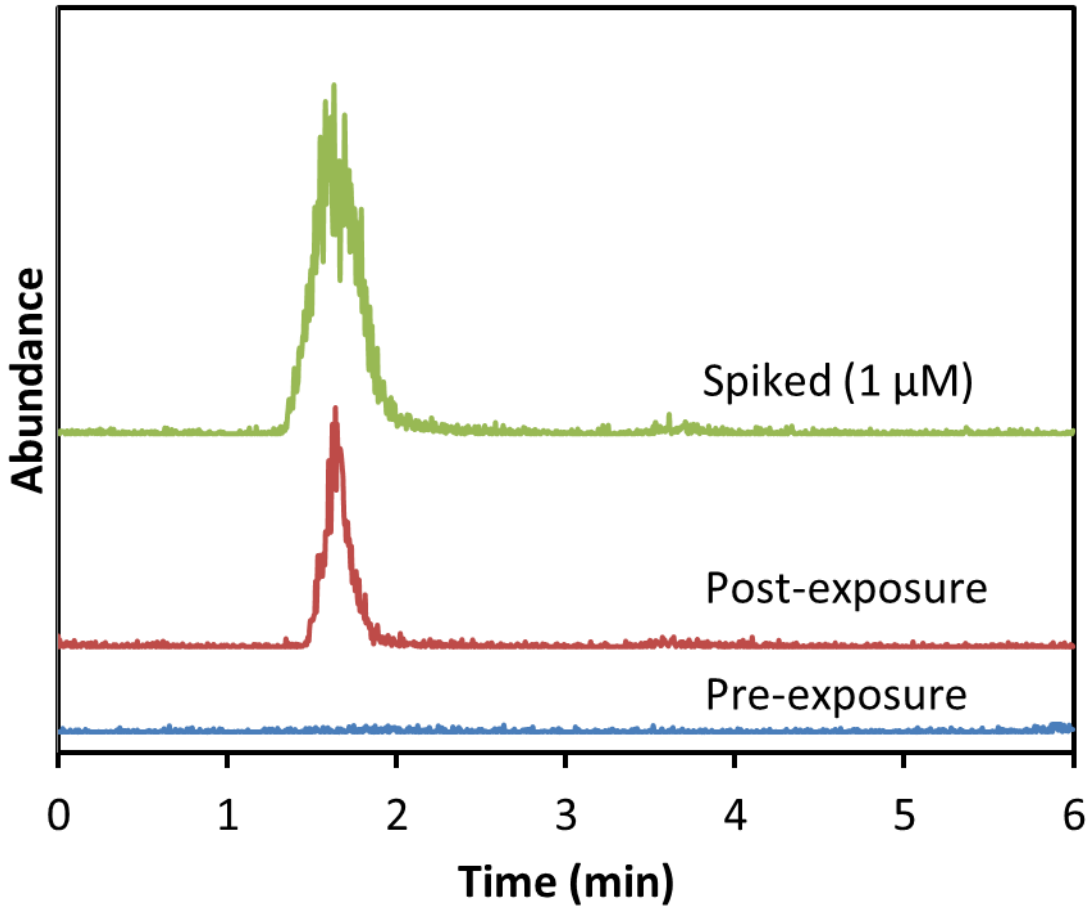

Figure 2.5-2. Chromatograms of α-KgCN spiked swine plasma (upper trace) and the plasma of cyanide-exposed swine, pre-exposure (lower trace), and post-exposure (middle trace).

Toxicokinetic Behavior of α-KgCN in Swine

The toxicokinetic behavior of α-KgCN was evaluated in potassium cyanide-exposed swine and compared with that of cyanide and its detoxification products, thiocyanate and ATCA.

Potassium cyanide-exposed swine plasma was obtained from Wilford Hall Medical Center (Lackland Air Force Base, TX)[8]. Ten animals (about 50 kg each) were sedated, endotracheally intubated, and anesthetized (with isoflurane). KCN (4 mg/mL) was infused by IV (0.17 mg/kg/min) until apnea. Arterial blood was sampled (20 mL per time point) prior to exposure, 5 min after the start of cyanide infusion, at apnea, and at 2, 4, 6, 8, 10, 20, 30, 40, 50, and 60 min post-apnea. An aliquot of the whole blood (4 mL) was then placed into EDTA centrifuge tubes and centrifuged to separate the plasma from the red blood cells. After centrifugation, the plasma (1 mL/sample) was removed and shipped on ice to South Dakota State University. Upon receipt, the plasma was frozen and stored at -80 ^{o}C until needed. The animal studies were conducted in accordance with the guidelines outlined in *The Guide for the Care and Use of Laboratory Animals.* The research facility where the animal studies were performed was accredited by AALAS (American Association for Laboratory Animal Science) and approved by the appropriate institutional review board.

The behavior of α-KgCN, ATCA, cyanide, and thiocyanate in untreated swine after cyanide exposure is shown in Figure 2.5-3. The general shape of the concentration versus time curves for cyanide, ATCA, and α-KgCN are similar, with the exception that cyanide levels are considerably higher compared to ATCA and α-KgCN. Plasma concentrations of ATCA and α-KgCN both increased as cyanide was infused and decreased following apnea, although ATCA does not decrease as rapidly as α-KgCN, likely because ATCA formation is not an equilibrium reaction, as is production of α-KgCN. Thiocyanate behaved quite differently compared to the other cyanide

exposure markers. Thiocyanate concentrations decreased directly after apnea (2 and 4 min) and then rose gradually for the duration of the experiment.

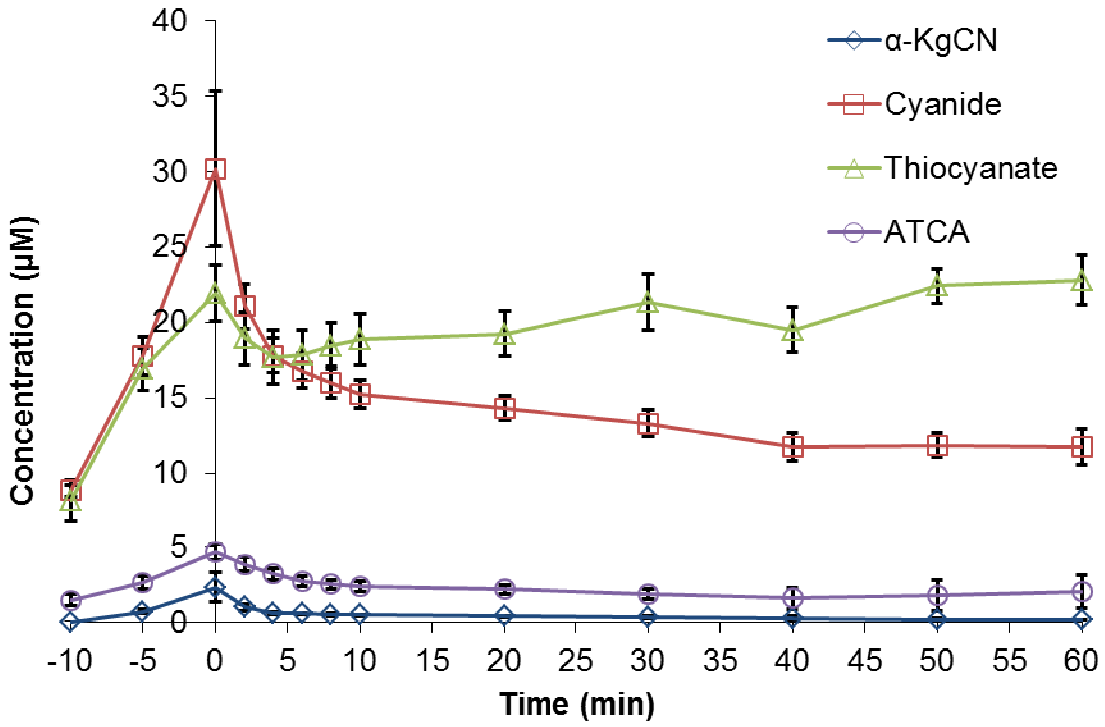

Figure 2.5-3. Plasma concentrations (µM) of α-KgCN, cyanide, thiocyanate, and ATCA in untreated swine over time (min). Apnea, pre-exposure and 5 min infusion sample points are designated as "time 0, -10, and -5", respectively. The plasma sampled at time zero was gathered prior to treatment, the -10 time point was obtained before infusion and the -5 time point was collected 5 min after exposure. Error bars denote SEM.

Based on this study, the use of α-KgCN as a biomarker for cyanide would be most applicable in instances of acute, high-dose cyanide poisoning soon after exposure in untreated individuals. Upon comparison of the cyanide, thiocyanate, ATCA and α-KgCN plasma levels (Figure 2.5-3) to the endogenous (baseline) concentrations of

these detoxification products, α-KgCN showed a 102.2-fold increase in signal response compared to the baseline concentrations. This value is significantly higher than cyanide, ATCA, or thiocyanate (2.8 times the baseline), which suggests that a definitive confirmation of cyanide exposure by analyzing α-KgCN in plasma is plausible. The major advantage of using α-KgCN as a marker for cyanide exposure is the low, if not undetectable, levels of endogenous α-KgCN in the plasma, making cyanide exposure easy to detect from elevated α-KgCN concentrations.

CONCLUSIONS AND FUTURE WORK

An analytical method for the determination of an alternative marker of cyanide exposure was evaluated. This method shows the ability to detect α-KgCN in swine plasma at low concentrations as indicated by the LOD. Furthermore, α-KgCN can be quantified accurately and precisely in swine plasma, at sub-micro molar concentrations as indicated by the LLOQ. This should allow α-KgCN to serve as a biological marker for cyanide exposure and aid in therapeutic treatment studies of cyanide with α-Kg by analysis of α-KgCN. To our knowledge, the method developed here is the first reported analytical method for detecting the cyanide metabolite, α-KgCN, in any matrix[9].

This investigation was completed and a manuscript detailing the method has been accepted for publication[10].

REFRENCES

1. Simeonova, F. P.; Fishbein, L. 2004. Hydrogen cyanide and cyanides: human health aspects. *Concise Int Chem Assess Doc 61*, i-iv, 1-67.

2. Szinicz, L. 2005. History of chemical and biological warfare agents. *Toxicol 214*, 167-181.

3. Baskin, S. I.; Brewer, T. 1997. *Textbook of Military Medicine, Medical Aspects of Chemical and Biological Warfare*; Borden Institute.

4. Lundquist, P.; Rosling, H.; Sorbo, B.; Tibbling, L. 1987. Cyanide concentrations in blood after cigarette smoking, as determined by a sensitive fluorimetric method. *Clin Chem 33*, 1228-30.

5. Flora, S. J. S.; Romano, J. A.; Baskin, S. I.; Sekhar, K. 2004. Editors: *Pharmacological Perspectives of Toxic Chemicals and Their Antidotes*; Springer GmbH.

6. Norris, J. C.; Utley, W. A.; Hume, A. S. 1990. Mechanism of antagonizing cyanide-induced lethality by α-ketoglutaric acid. *Toxicol 62*, 275-83.

7. Wagner, B. M.; Donnarumma, F.; Wintersteiger, R.; Windischhofer, W.; Leis, H. J. 2010. Simultaneous quantitative determination of α-ketoglutaric acid and 5-hydroxymethylfurfural in human plasma by gas chromatography-mass spectrometry. *Anal Bioanal Chem 396*, 2629-2637.

8. Bebarta, V. S.; Tanen, D. A.; Lairet, J.; Dixon, P. S.; Valtier, S.; Bush, A., 2010. Hydroxocobalamin and sodium thiosulfate versus sodium nitrite and sodium thiosulfate in the treatment of acute cyanide toxicity in a swine (Sus scrofa) model. *Annals of Emergency Medicine* 55 (4), 345-51.

9. Mitchell BL, Rockwood GA, Logue BA. Quantification of cyanide metabolite α-ketoglutarate cyanohydrin in plasma by ultra high-performance liquid chromatography tandem mass spectrometry. *J. Chromatogr. B (Manuscript accepted).*

10. Mitchell B.L., Bhandari R.K., Bebarta V.S., Rockwood G.A., Boss G.R., and Logue B.A. 2013. Toxicokinetic profiles of α-ketoglutarate cyanohydrin, a cyanide detoxification product, following exposure to potassium cyanide. *Toxicology Letters (Manuscript accepted).*

CHAPTER 6

DETERMINATION OF THE CYANIDE ADDUCT OF GLUTATHIONE BY HIGH PERFORMANCE LIQUID CHROMATOGRAPHY

Wenhui Zhou, Robert P. Oda and Brian A. Logue

INTRODUCTION

Glutathione (GSH) is the primary intra-cellular reducing agent, and is active in many metabolic processes, including the detoxification of xenobiotics and removal of peroxides[1]. In maintaining the oxidative state of the cell, glutathione reduces disulfides to thiols, while becoming oxidized to the glutathione homo-disulfide (or glutathiol, GSSG). Although intra-cellular levels of glutathione may range from 1-10 mM, the extra-cellular levels are low[1,2]. Within blood, most of the glutathione is contained within the erythrocytes, where it may reach mM concentrations[2-4]. However, circulating extra-cellular GSSG concentrations may be as high as 200 µM in plasma, while glutathione levels are in the 2-5 µM range[2-4]. The detoxification of cyanide with GSH or GSSG may be a first-line defense against cyanide intoxication, as studies have demonstrated a reduced toxicity of cyanide in glutathione and glutathione-disulfide-pretreated mice[5]. Although the mechanism of toxic reduction is unknown, it is possible that the reaction of cyanide with circulating GSH or GSSG might reduce the availability of cyanide to produce cellular toxicity.

Protein-bound thiocyanate ion was released from serum proteins following reaction with cyanide[6,7], which demonstrated that the disulfide bond would react with

cyanide under alkaline conditions. GSSG might react with cyanide, since it contains a reactive disulfide bond. Therefore, we investigated the possibility of a non-enzymatic cyanide reaction with GSH and/or GSSG, producing adduct(s) which might serve as a bio-marker(s) for cyanide exposure.

Cyanamide was used to create a possible GS-CN adduct analogous to the reaction by Nagasawa[8] to create ATCA from cysteine for use as a standard compound. Possible adducts from the reaction of GSH with cyanamide are depicted in Figure 2.6-1. Possible products from the reaction of GSSG with CN are depicted in Figure 2.6-2. It should be noted that the initial products from the reaction depicted in Figure 2.6-2 could undergo the rearrangements pictured in Figure 2.6-1.

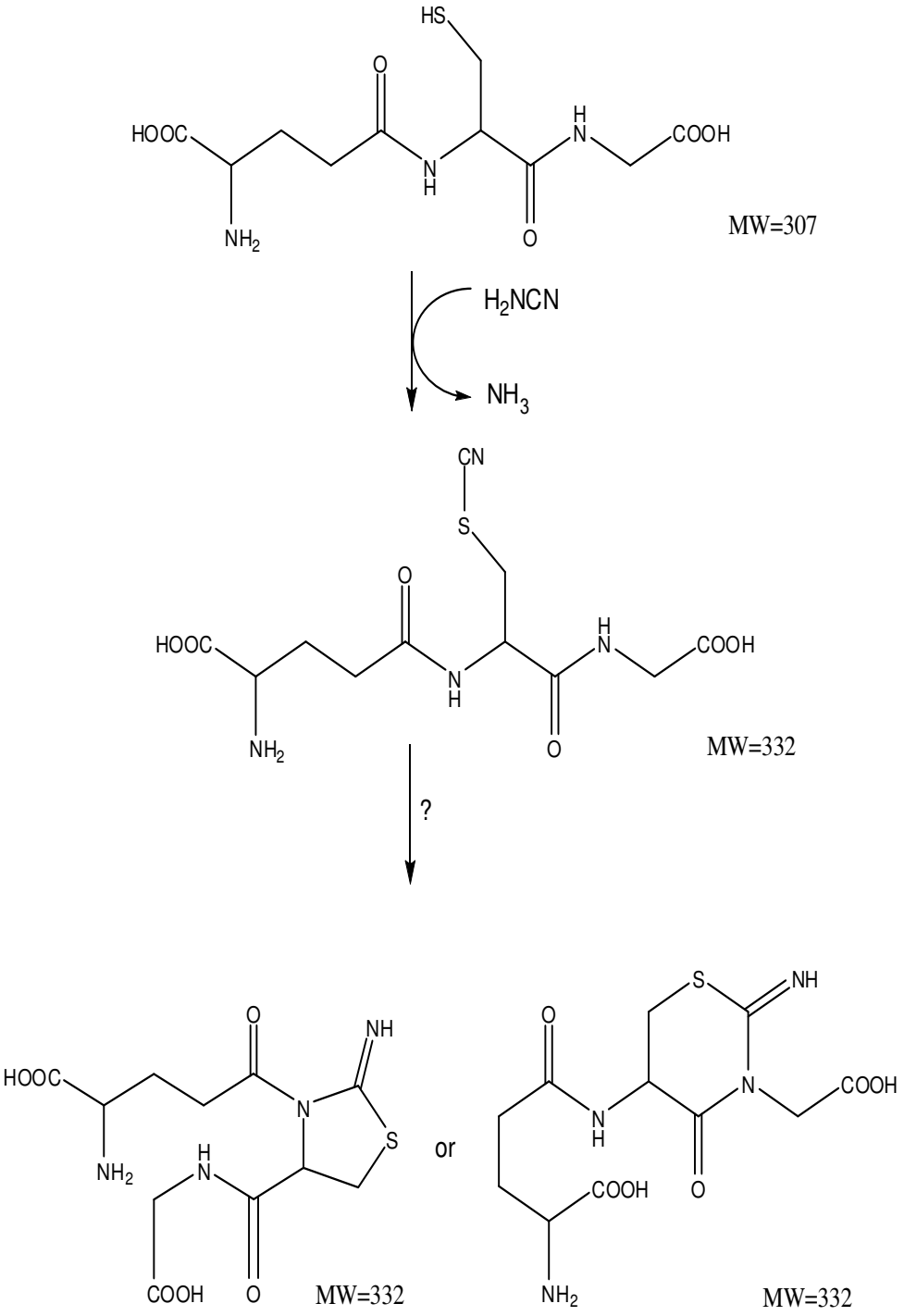

Figure 2.6-1. Reaction scheme for the condensation of cyanamide with reduced glutathione (GSH), and possible rearrangement of the initial product.

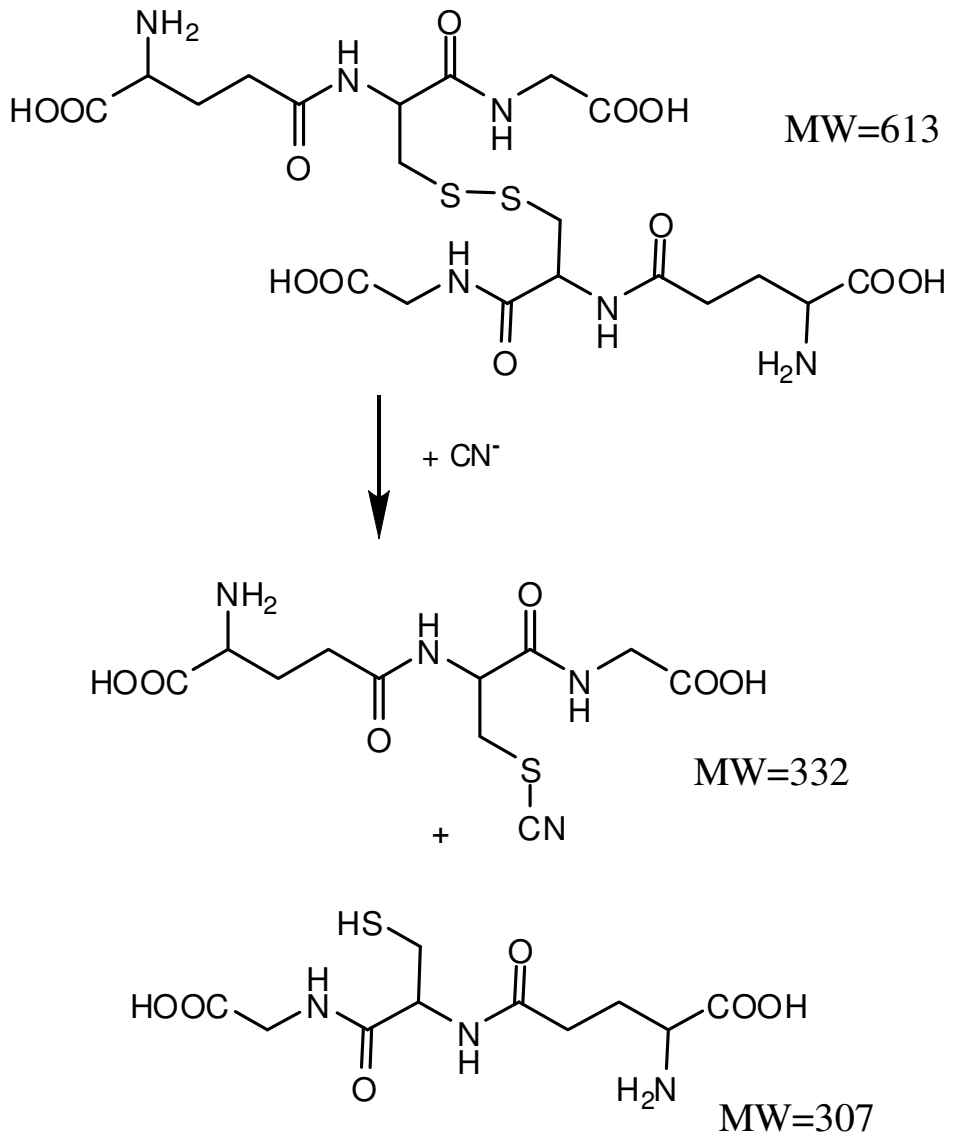

Figure 2.6-2. Reaction scheme for the addition of cyanide to oxidized glutathione (GSSG), and possible products.

EXPERIMENTAL

Reagents and Materials

All reagents were at least reagent grade. Sodium cyanide (NaCN), sodium phosphate salts, and methanol (HPLC grade) were purchased from Fisher Scientific (Fair Lawn, NJ, USA). Glutathione (reduced, GSH), ammonium formate, Ellman's reagent, ninhydrin, monobromobimane, and sodium carbonate were products of Sigma-Aldrich (St. Louis, MO, USA). LC/MS grade formic acid and Ellman's Reagent [5, 5'-dithio-bis(2-nitrobenzoic acid)] were purchased from Thermo Scientific (Rockford, IL, USA). Reverse-osmosis water was passed through a polishing unit and had a conductivity of 18.2 M-Ω.

Oxidized glutathione (glutathiol, GSSG) was produced by taking 50 mL of a 1 mM solution of glutathione (GSH) in 0.1 M phosphate buffer, pH 7.27, and adding 5 mL 3% hydrogen peroxide drop-wise over several minutes with constant stirring. The lack of reaction with Ellman's reagent was used as an indicator for completion of the reaction. In later experiments, GSH (61.4 mg; 200 mmoles) was dissolved in 10 ml water to which 15 drops of 3% hydrogen peroxide was added over several minutes with constant stirring.

Preparation of Cyanide Adducts

Aliquots (1 mL of 1 mM solution) of glutathione or glutathione-disulfide in phosphate buffer (pH 7.27), borate buffer (pH 8.3 and 9.25), or sodium carbonate (pH 10.6) were mixed with a cyanide solution in a 1:10 or 1:20 molar ratio to present a ten-

fold molar excess ratio of cyanide to sulfur and allowed to react for up to 2 hours at room temperature. The reaction mixtures were assayed for the presence of CN- adducts by HPLC. The high salt content of the reaction mixture required the samples to be diluted or dialyzed to reduce the salt load onto the HPLC column. This was best accomplished by "float dialysis", in which an aliquot (200 µL) of reaction mixture was placed on a 0.2 µ 47 mm nylon filtration membrane (Millipore, Billerica, MA, USA) floated on about 20 mL deionized water. After 10 minutes of dialysis, the residual sample was filtered through a 0.2 µ filter into a 150 µL insert in a 2 mL vial, capped, and analyzed by HPLC.

Assay of Free Thiols with Ellman's Reagent [9,10]

An aliquot of sample (0.1 mL) was mixed with an equal volume of 0.1 M sodium phosphate buffer, pH 7.27, to which was added 0.1 mL Ellman's reagent (5, 5'-dithio-bis(2-nitrobenzoic acid), 1.7 mM) in phosphate buffer, pH 7.27, containing 0.1 mM EDTA. The yellow product was analyzed at 412 nm.

Mass Spectrum Analysis

A Thermoquest Finnigan LCQ Deca Mass Spectrometer (Thermo Scientific, Waltham, MA, USA) with a turbo electrospray ion source was used to screen the GSH – cyanamide and GSSG-cyanide reactions for products. A 5500 Q-Trap (Applied Biosystems, Foster City, CA, USA) was used for MS-MS analysis of presumed cyano-

adducts. Samples from the original reaction mixtures and various extraction solutions and collected fractions were analyzed as appropriate.

Reverse Phase-High Performance Liquid Chromatography

HPLC analysis was performed on an Agilent 1200 HPLC system consisting of a quaternary pump, auto-sampler, vacuum degasser, multi-wavelength detector, and a fluorescence detector (Agilent Technologies, Wilmington, DE, USA). A Discovery Bio wide pore C-18 column (150 mm x 2.1 mm i.d.; 5-µm particle size; Supelco, Bellfonte, PA, USA) and a mobile phase containing 0.1% formic acid (Pierce Chemical, Rockforf, IL, USA) was used to separate the analytes at a flow rate of 0.350 mL/min. 0.1% Formic acid in methanol was used in a gradient elution from 10% (held for 1 min), linearly increased to 100% over 21 min and held for 2 min. The mobile phase was then linearly converted to the initial composition over 2 min and subsequently held for 2 min prior to the next analysis. A multi-wavelength detector monitored absorbance at 270 nm.

In later experiments a Zorbax C-18 column (150 mm x 4.6 mm i.d.; 5-µm particle size; Agilent Technologies, Wilmington, DE, USA) with a flow rate of 1.00 mL/min were used. The mobile phase consisted of 1 mM ammonium formate, pH 4.0 in water. Methanol containing 1 mM ammonium formate, pH 4.0 was used in a gradient elution from 0% (held for 3 min), linearly increased to 20% over 2 min, to 40% over 10 min, to 100% over 2 min and held at 100% for 3 min. The mobile phase was then linearly decreased to the initial composition over 2 min and subsequently held for 3 min prior to the next analysis. A multi-wavelength detector monitored absorbance at 230 and/or 270

nm. Fluorescent monobromo-bimane reaction products were excited at 390 nm and the emission was monitored at 490 nm.

RESULTS AND DISCUSSION

A glutathione adduct was prepared by a procedure adapted from Nagasawa[8]. GSH (3 g) was mixed with 0.822 g sodium bicarbonate, and placed under a nitrogen atmosphere. Cyanamide (0.4287 g) and water (15 mL) were added to dissolve the mixture, and the mixture refluxed for five hours. The reaction mixture was separated by using a normal-phase silica gravity column. Different chloroform/methanol solvent mixtures from 0% to 100% were used to elute compounds from the column. A mobile phase of 50% methanol in water was then used to elute highly polar compounds. Fractions were collected and analyzed by HPLC. The peak at 3.87 minutes in the chromatogram of the reaction mixture in Figure 2.6-3 was presumed to be main product from the GSH-cyanamide reaction. Fraction 8, from 20% methanol in chloroform, has a single peak which eluted at 1.72 minutes (Figure 2.6-3), was presumed to be unreacted GSH by comparison of the retention time of an aqueous solution of GSH. Fractions 11 and 12 were eluted by 50% methanol in water. Fraction 11 displayed two early eluting peaks (Figure 2.6-4) which appear to be GSSG and GSH by comparison of retention times with standard aqueous solutions. Fraction 12 has two peaks. The first peak (1.5 min) elutes with the retention time of GSSG. The second peak which eluted at 3.37

minutes may be the desired product (Figure 2.6-4), but did elute prior to the peak identified in the reaction mixture. More work must be done to identify this peak.

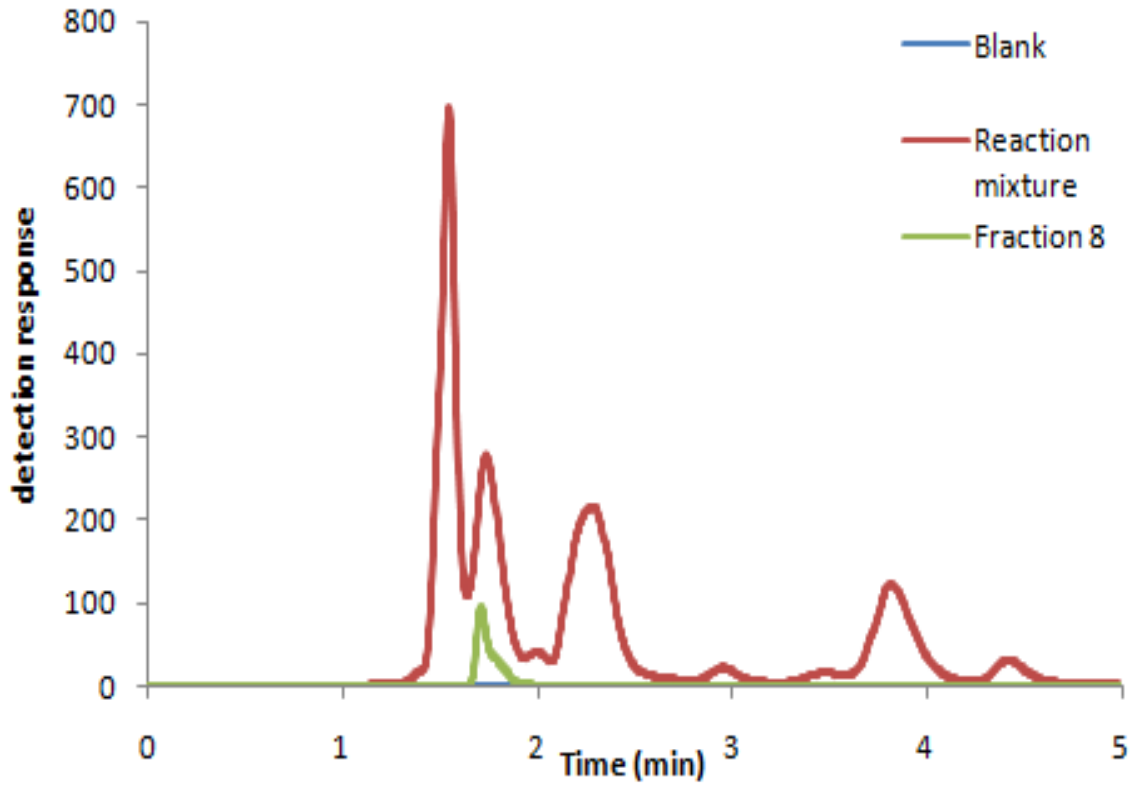

Figure 2.6-3. Overlaid HPLC chromatograms of a reagent blank, the reaction mixture from GSH and cyanamide, and Fraction 8 eluted by 20% methanol in chloroform solvent from the silica column. HPLC conditions: Column: Zorbax C-18, 4.6 X 150 mm; Mobile phase: 1mM ammonium formate in water/ methanol; Flow: 1.0 mL/ min; Detection: 270 nm.

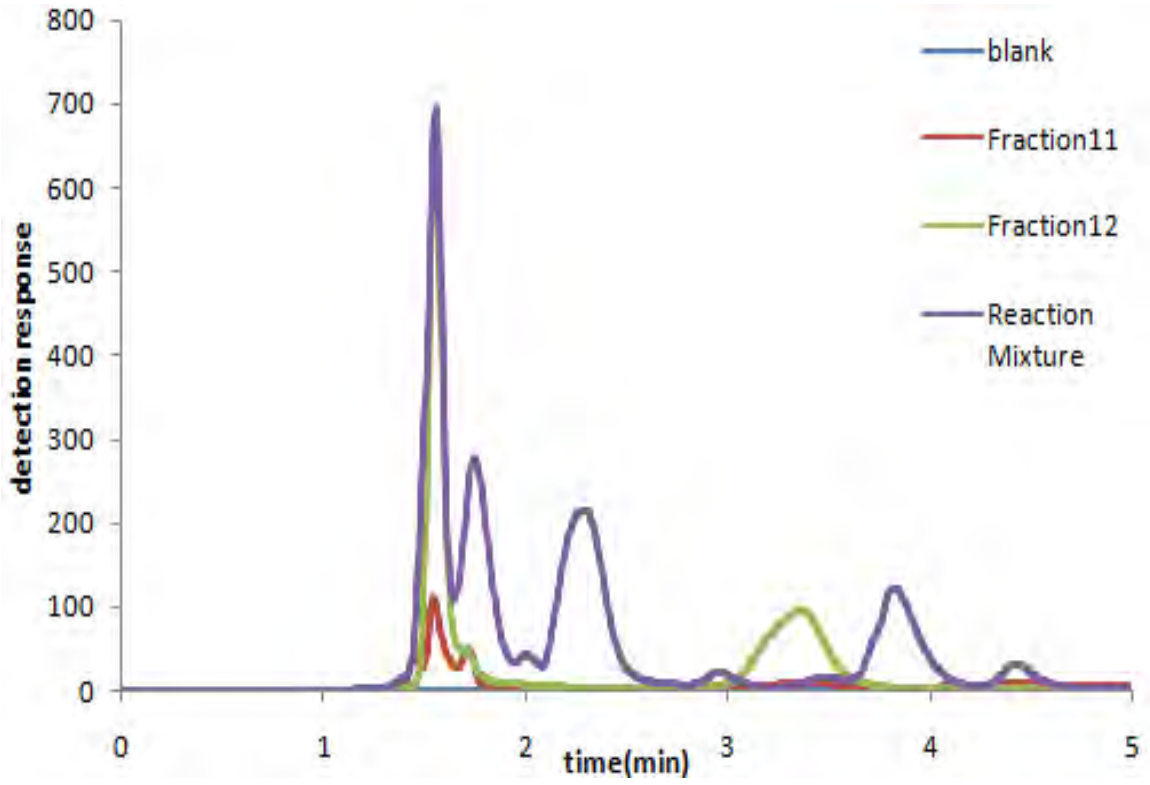

Figure 2.6-4. Overlaid HPLC chromatograms of a reagent blank, the reaction mixture from GSH and cyanamide, and Fractions 11 and 22 eluted by 50% methanol in water from the silica column. HPLC conditions: Column: Zorbax C-18, 4.6 X 150 mm; Mobile phase: ammonium formate (1 mM) in water/methanol; Flow: 1.0 mL/ min; Detection: 270 nm.

Swine plasma (1 mL) was spiked with 6.5 mg KCN and 65.2 mg KCN separately to form 10 mM and 100 mM cyanide-spiked plasma. After a couple of hours' reaction, acetone (3 mL) was added to the sample to precipitate proteins, and the sample kept at 4°C for 15 minutes. The samples were then centrifuged for 10 minutes at 10,000 RPM ($9.6x10^3$ x g), the supernatants were removed and dried with N_2 gas, and reconstituted with 2 mL buffer (1% NH4OOCH in water). Samples were then filtered (0.22 µm PVDF filter) and analyzed by LC-MS.

High-performance liquid chromatography-tandem mass spectrometry (UHPLC-MS) conducted on a Shimadzu HPLC (LC-20AD, Shimadzu Corp., Kyoto, JPN) coupled to an AB Sciex Q-Trap 5500 MS (Applied Biosystems, Foster City, CA, USA). Samples were separated by reversed-phase (RP) chromatography using a Phenomenex Synergi 4µ RP Max column (2.0 x 50mm) (Phenomenex, Torrance, CA, USA) as a stationary phase. A mobile phase containing 1 mM ammonium formate (Sigma-Aldrich, St. Louis, MO, USA) was used at a flow rate of 0.25 mL/min. Methanol was used in a gradient elution from 0% (held for 3 min), linearly increased to 20% over 2 min, to 40% over 10 min, to 100% over 2 min and held at 100% for 3 min. The mobile phase was then linearly decreased to the initial composition over 2 min and subsequently held for 3 min prior to the next analysis.

Mass spectrometry was used to assess if there was a putative product in the reaction mixture. The spectra of the reaction mixtures of cyanide-spiked plasma (10 µM and 100 µM) are pictured in Figure 2.6-5. The peaks at m/z = 213 and 279 from the 100 mM reaction mixture were higher than those in the 10 mM solution and are presumed to be the putative product(s) of the reaction. Further analysis is required to confirm the identity of these peaks. Possible structures for the presumed products are depicted in Figure 2.6-6a and b.

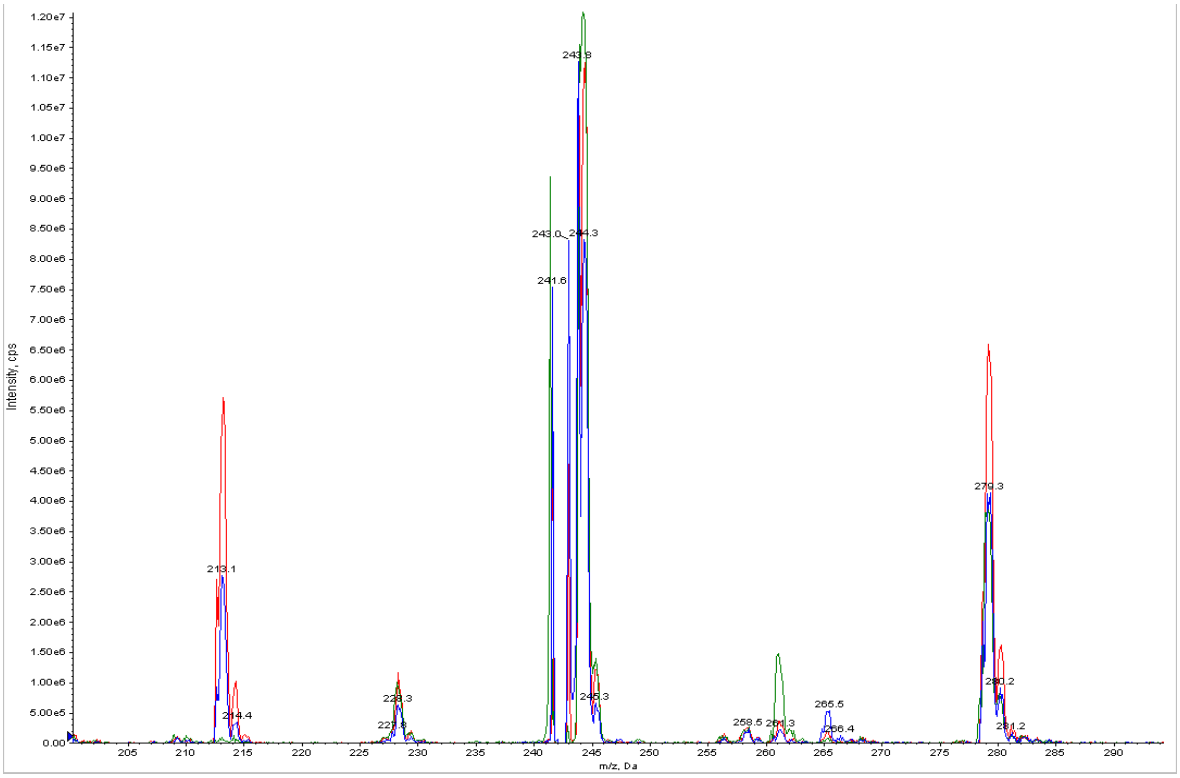

Figure 2.6-5. Overlaid mass spectra of the cyanide-spiked plasma reaction mixtures. 100 mM CN (red) , 10 mM CN (green) and a plasma blank (blue). AB Sciex Q-trap 5500 Mass Spectrometer in positive ion mode with an ESI source.

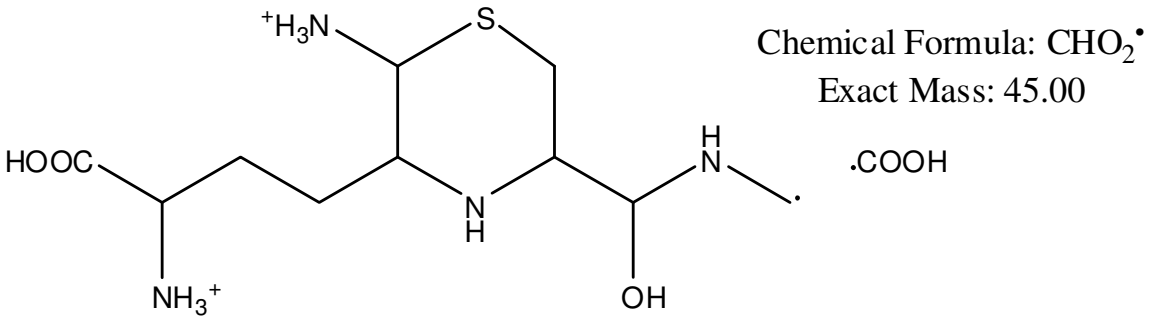

Chemical Formula: $CHO_2^{\bullet}$
Exact Mass: 45.00

Chemical Formula: $C_{10}H_{23}N_4O_3S^{\bullet 2+}$
Exact Mass: 279.15

Figure 2.6-6a. Possible structure for the observed m/z = 279 fragment.

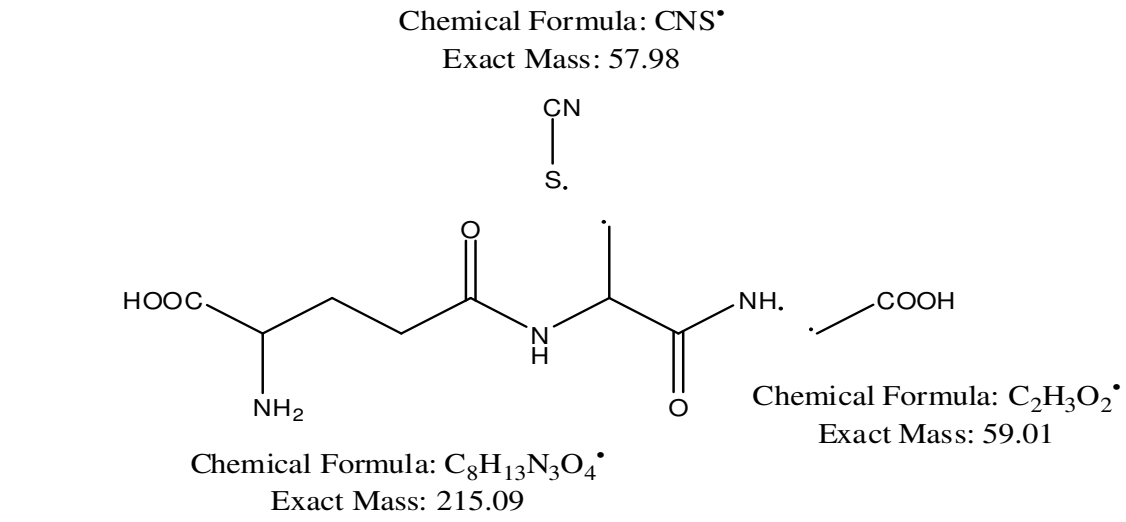

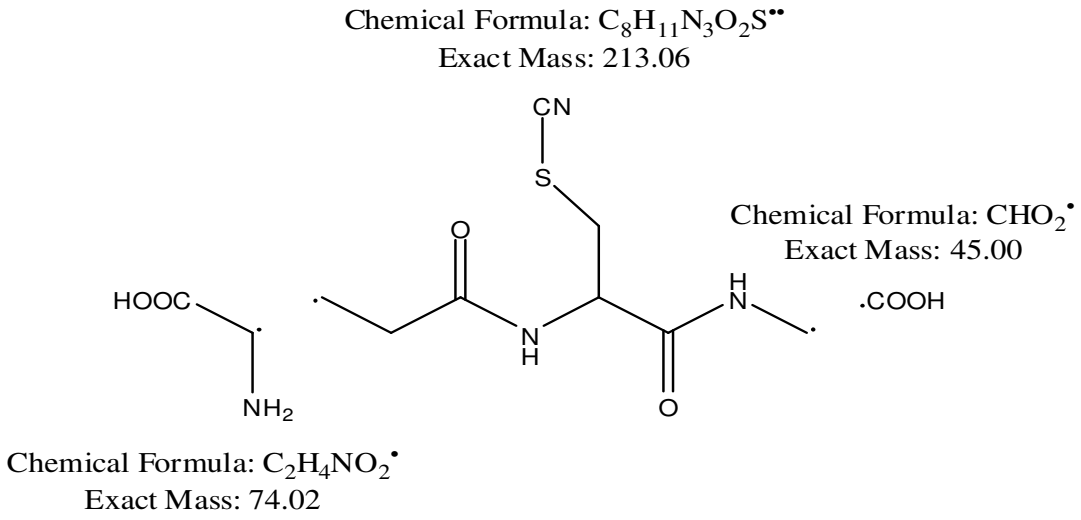

Figure 2.6-6b. Possible structures for the m/z = 213 fragment.

For the determination of the glutathione-cyanide adducts, there are numerous by-products from the reaction which make the interpretation of structural and

chromatographic information difficult. The use of the LC-MS should enable the putative adducts to be resolved and characterized.

The person most responsible for this project has left the laboratory. Therefore, minimal progress was made on this project.

REFERENCES

1. Meister, A. and Anderson, M. E., 1983. Glutathione. *Ann Rev Biochem* 52, 711-760.

2. Jose, C. J., Jacob, R. H., Gardner, G. E., Pethick, D. W., and Liu, S. M., 2010. Selenium supplementation and increased muscle glutathione concentration do not improve the color stability of lamb meat. *J Agric Food Sci* 58 (12), 7389-7393.

3. Serru, V., Baudin, B., Ziegler, F., David, J-P., Cals, M-J., Vaubourdolle, M., and Mario, N., 2001. Quantification of reduced and oxidized glutathione in whole blood samples by capillary electrophoresis. *Clin Chem* 47 (7), 1321-1324.

4. Michelet, F., Gueguen, R., Leroy, P., Wellman, M., Nicolas, A., and Siest, G., 1995. Blood and plasma glutathione measured in healthy subjects by HPLC: Relation to sex, aging, biological variables, and life habits. *Clin Chem* 41 (10), 1509-1517.

5. Hatch, R. C., Laflamme, D. P., and Jain, A. V., 1990. Effects of various known and potential cyanide antagonists and a glutathione depletor on acute toxicity of cyanide in mice. *Vet Human Toxicol* 32 (1), 9-16.

6. Catsimpoolas, N., and Wood, J. L., 1964. The reaction of cyanide with bovine serum albumin. *J Biol Chem* 239 (12), 4132-4137.

7. Youso, S. L., Rockwood, G. A., Lee, J. P., Logue, B. A., 2010. Determination of cyanide exposure by gas chromatography-mass spectrometry analysis of cyanide-exposed plasma proteins. *Anal Chim Acta* 677 (1), 24-28.

8. Nagasawa, H. T., Cummings, S. E., and Baskin, S. I., 2004. The structure of "ITCA", a urinary metabolite of cyanide. *Organic Prep and Proc Int'l* 36 (2), 178-182.

9. Ellman, G. L., 1959. Tissue sulfhydryl groups. *Arch Biochem Biophys* 82, 70-77.

10. Habeeb, A. F. S. A., 1972. Reaction of protein sulfhydryl groups with Ellman's reagent. *Methods Enzymol.* 25 (part B), 457-464.

CHAPTER 7

DEVELOPMENT OF AN ASSAY FOR DIMETHYL TRISULFIDE, A POTENTIAL THERAPEUTIC AGENT AGAINST CYANIDE TOXICITY

Wenhui Zhou and Brian A. Logue

2.7. Determination of the DMTS by Liquid Chromatography-Mass Spectrum

Cyanide has figured as a prominent human toxicant over the years as a result of both accidental and intentional exposure. Within the purview of cyanide detoxification, DMTS was shown to effectively function as sulfur donor for rhodanese *in vitro*[1]. In addition, it was demonstrated that DMTS by itself is a very efficient converter of cyanide to thiocyanate [2-4]. Thus, an assay for detecting DMTS would be necessary should it become useful as a therapeutic agent.

EXPERIMENTAL

DMTS (0.5 mM) was spiked with NaBr (0.1mM) to form a possible adduct. The sample was then filtered (0.22 µm PVDF filter). Mass spectrometry was used to assess if there was a putative adduct in the solution.

A Shimadzu UHPLC (LC 20A Prominence, Kyoto, Japan) coupled to a 5500 Q-Trap mass spectrometer (AB Sciex, Framingham, MA, USA) along with an electrospray ion source was used to for HPLC-MS-MS analysis. Separation was performed on a

Phenomenex Synergy Fusion RP column (50 x 2.0 mm, 4 µm 80Å) with an injection volume of 10 µL from samples kept in a cooled autosampler (15°C). Mobile phase solutions consisted of 5mM aqueous ammonium formate with 10% methanol (Mobile Phase A) and 5mM ammonium formate in 90% methanol (Mobile Phase B). A gradient of 0 to 100%B was applied over 3 min, held constant for 0.5 min, then reduced to 0% B over 1.5 min. The total run-time was 5.1 min with a flow rate of 0.25 mL/min. The turbo ion-spray interface was kept at 500°C with zero air nebulization at 90 psi in negative mode with drying and curtain gasses held at 60 psi each. The declustering potential was -101.56.

Analysis of DMTS was performed by headspace on an Agilent GC-MS system (Agilent Technologies, Wilmington, DE, USA) consisting of a 6890N series gas chromatograph, a 5975 series mass detector, and a Gerstel MPS sampler (Gerstel Inc., Linthicum, MD, USA). A DB5-MS bonded-phase column (30 m x 0.25 mm I.D., 0.25 µm film thickness; J&W Scientific, Folsom, CA, USA) was used with nitrogen as the carrier gas at a flow rate of 1.0 mL/min and a column head pressure of 10.0 psi. An aliquot (50 µL) of solution containing DMTS was placed in a 20 mL headspace vial with a Teflon-lined septum. The vial was incubated at 115 °C for up to 5 min, before a 100 µL sample was withdrawn. The auto-sampler injected a 100 µL headspace sample into the splitless injection port which was held at 120 °C. A deactivated, straight-through glass inlet liner packed with about 1 cm of glass wool was used. The GC oven temperature was initially held at 30 °C for 2 min, then elevated at a rate of 15 °C/min up to 120 °C. The gradient was increased to 120 °C/min up to 300 °C where it was held constant for 1.5 min, before returning to the initial temperature. The injection syringe temperature

was 115 °C. The GC was interfaced with a mass selective detector with electron ionization. Selective-ion-monitoring (SIM) mode was used, detecting ions with m/z of 79, 94, 111, and 126. DMTS was identified at m/z = 126/111 and DMDS by m/z = 94/79.

In an initial experiment, DMTS was spiked into rabbit plasma. An aliquot of plasma (900 µL) was spiked with 100 µL DMTS (in methanol) to make a final concentration of 1 mM. An aliquot (50 µL) was taken for assay by GC/MS headspace.

RESULTS AND DISCUSSION

The spectra of the solution mixtures of NaBr-DMTS (0.5 mM and 1 mM) are pictured in Figure 2.7-1. The peak at m/z = 119 is presumed to be the putative adduct (might be CH_3-NaBr).

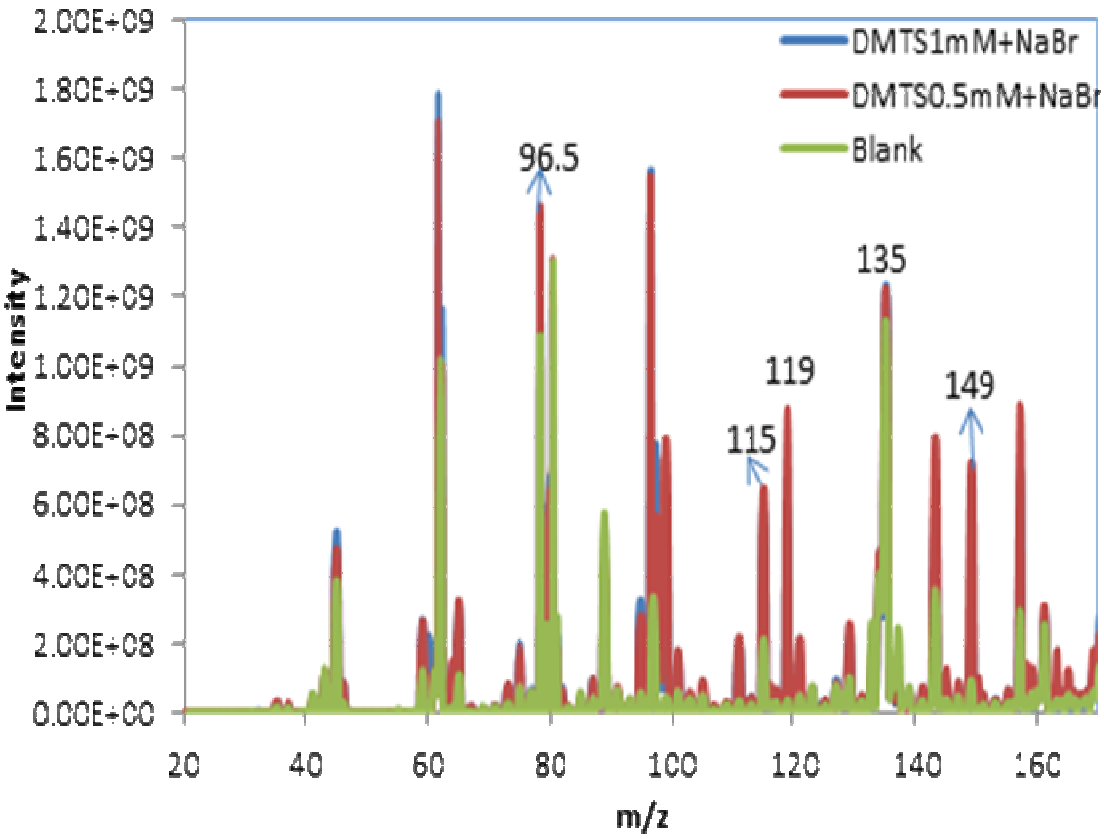

Figure 2.7-2. Overlaid mass spectra of the DMTS-spiked NaBr solution mixtures. 0.5 mM DMTS (red), 1 mM DMTS (blue) and a NaBr blank (green). AB Sciex Q-trap 5500 Mass Spectrometer in negative ion mode with an ESI source.

Multiple-reaction-monitoring (MRM) transitions of 119→95.8 and 119→80.0 m/z (95.8 could be 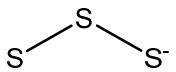 ; 80 could be Br, 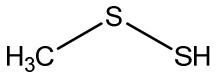) were used with collision energy of -29.41 and -48.47 V, respectively. The dwell time was 100 ms for both transitions. Analyst software (Applied Biosystems version 1.5.2) was used for data acquisition and analysis. The chromatogram of the DMTS is shown in Figure 2.7-2. The results were inconclusive. There was no peak in neither 0.5mM DMTS-spiked

NaBr nor 1mM DMTS-spiked NaBr.(DMTS:NaBr = 5:1). We could try other columns, increase gradient, or look for other m/z values.

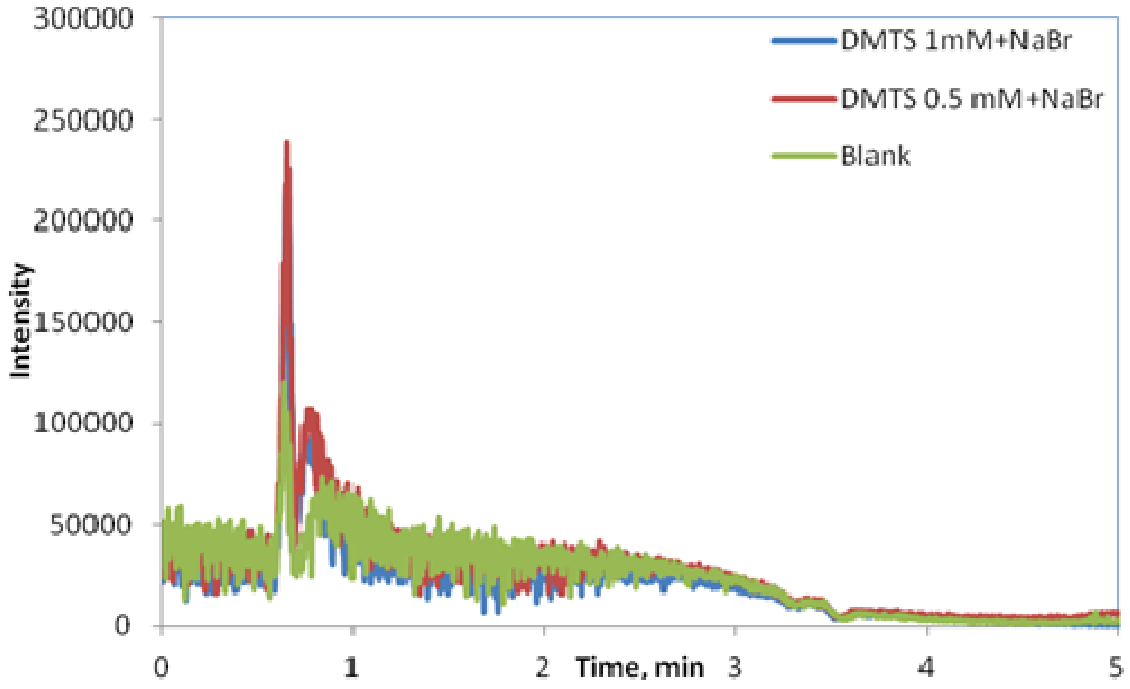

Figure 2.7-2. Overlaid chromatogram of the DMTS-spiked NaBr solution mixtures. 0.5 mM DMTS (red), 1 mM DMTS (blue) and a NaBr blank (green). AB Sciex Q-trap 5500 Mass Spectrometer in negative ion mode with an ESI source.

Different incubator temperatures were set to analyze DMTS in methanol; 115 ^{o}C was found to be the ideal incubator temperature (Figure 2.7-3). Syringe temperatures were also varied to optimize the method; 100 ^{o}C was found to be the best syringe temperature (Figure 2.7-4). The chromatogram of the DMTS-spiked blood was shown

in Figure 2.7-5. Based on the result, DMTS can be detected in blood. Compared with the same concentration of DMTS in methanol, DMTS was degraded in blood. Overall, a simple GC/MS headspace method for the analysis of DMTS from biological fluids was developed; however, it needs further optimization.

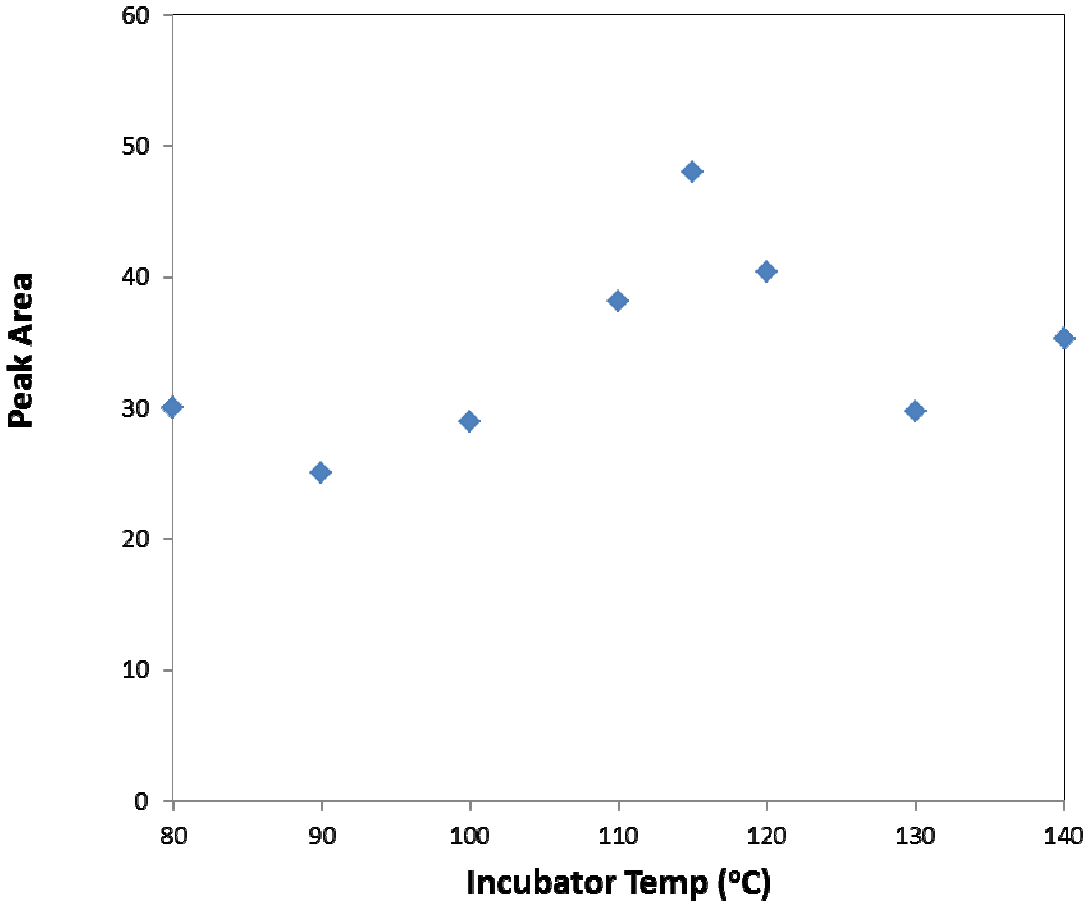

Figure 2.7-3. Average peak area of DMTS at different incubator temperatures.

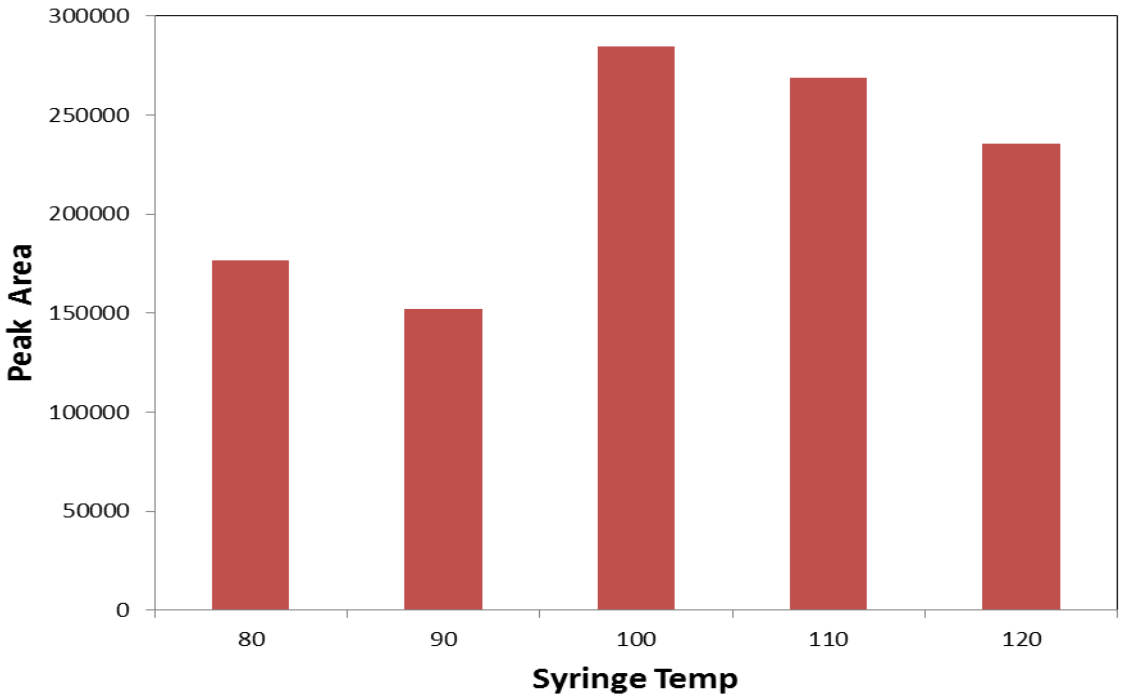

Figure 2.7-4. Average peak areas of DMTS at different syringe temperatures.

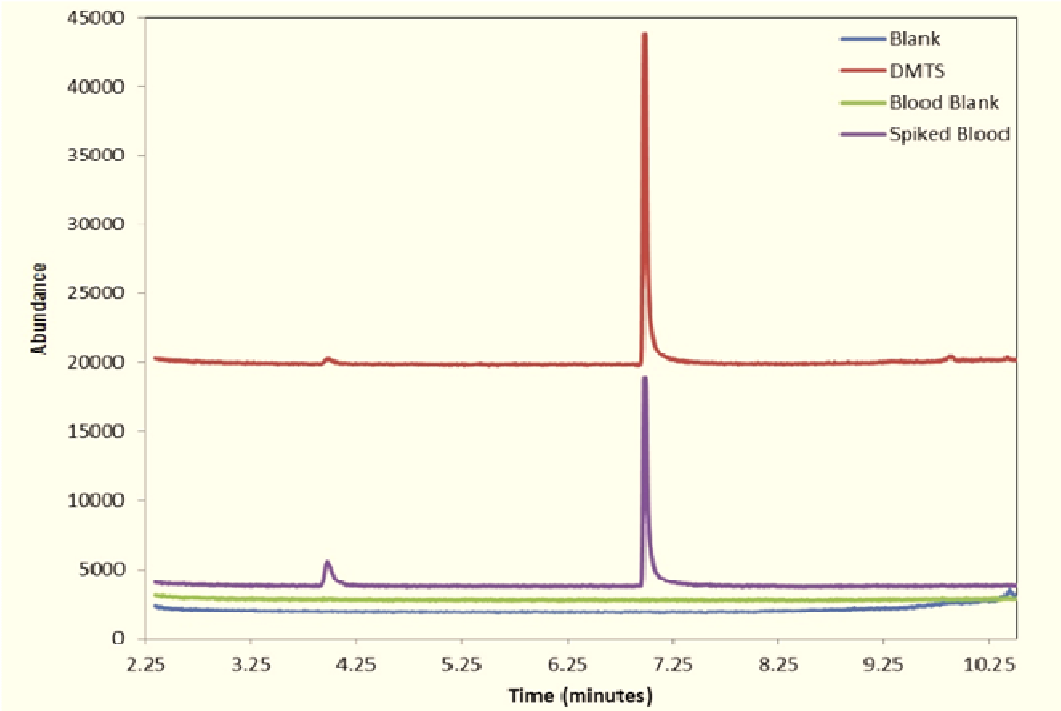

Figure 2.7-5. Overlaid chromatograms of 1 mM DMTS (red), DMTS-spiked blood (purple), blood blank (green) and a methanol blank (blue).

REFERENCES

1. Petrikovics I, Kuzmitcheva G, Budai M, Haines D, Nagy A, Rockwood GA, Way JL, 2010. Encapsulated rhodanese with two new sulfur donors in cyanide antagonism. In *XII International Congress of Toxicology*. Barcelona, Spain.

2. Frankenberg L, 1980. Enzyme therapy in cyanide poisoning: effect of rhodanese and sulfur compounds. *ArchToxicol* 45, 315-323.

3. Iciek M, Wlodek L, 2001. Biosynthesis and biological properties of compounds containing highly reactive, reduced sulfane sulfur. *Pol J Pharmacol* 53, 215-225.

4. Petrikovics I, Pei L, McGuinn W, Cannon E, Way J, 1994. Encapsulation of rhodanese and organic thiosulfonates by mouse erythrocytes. *Fund and Appl Toxicol* 23, 70-75.

BIBLIOGRAPHY

REFERENCES – INTRODUCTION

1. Strategic Plan and Research Agenda for Medical Countermeasures Against Chemical Threats (August, 2007), http://www.ninds.nih.gov/research/counterterrorism/counterACT_home.htm. Accessed 8/29/2012.

2. Youso, S. L. Rockwood, G. A. Lee, J. P. Logue, B. A. 2010 *Anal Chim Acta* 2010, 677, 24-28.

3. Logue, B. A.; Hinkens, D. M.; Baskin, S. I.; Rockwood, G. A. 2010 *Crit Rev Anal Chem* 44, 122-147.

REFERENCES –Chapter 1

1. Other Test Method 29 - Sampling and Analysis for Hydrogen Cyanide Emissions from Stationary Sources. EPA, Ed., 2011.

2. Ma, J. Dasgupta, P. K. Blackledge, W. Boss, G. R. 2010. Cobinamide-Based Cyanide Analysis by Multiwavelength Spectrometry in a Liquid Core Waveguide. *Anal Chem* 82, 6244-6250.

REFERENCES- Chapter 2

1. Logue, B. A. Hinkens, D. M. Baskin, S. I. Rockwood, G. A. 2010: The Analysis of Cyanide and its Breakdown Products in Biological Samples. *Crit Rev Anal Chem* 40, 122-147.

2. Logue, B. A. Kirschten, N. P. Petrikovics, I. Moser, M. A. Rockwood, G. A. Baskin, S. I. 2005. Determination of the cyanide metabolite 2-aminothiazoline-4-carboxylic acid in urine and plasma by gas chromatography-mass spectrometry. *J Chromatogr B: Analyt Technol Biomed Life Sci* 819, 237-44.

3. Baskin, S. Brewer, T. 1997. Cyanide poisoning. In *Medical Aspects of Chemical and Biological Warfare.* Sidell, F., Takafuji, E., Franz, D., Eds.; Office of the Surgeon General, Department of the Army, United States of America: Falls Church, Virginia, pp 271-286.

4. Baskin, S. I. Kelly, J. B. Maliner, B. I. Rockwood, G. A. Zoltani, C. K. 2008. Cyanide poisoning. In *Medical Aspects of Chemical Warfare.* Tuorinsky, S. D., Ed.; Office of the Surgeon General, Department of the Army, United States of America: Falls Church, Virginia, pp 371-410.

REFRENCES -Chapter 3

1. Bebarta, V. S. Tanen, D. A. Lairet, J. Dixon, P. S. Valtier, S. Bush, A. 2010. Hydroxocobalamin and sodium thiosulfate versus sodium nitrite and sodium thiosulfate in the treatment of acute cyanide toxicity in a swine (Sus scrofa) model. *Annals of Emergency Medicine* 55 (4), 345-51.

2. Bhandari, R.K., Oda, R.P., Youso, S.L., Petrikovics, I., Bebarta, V.S., Rockwood, G.A., Logue, B.A., 2012. Simultaneous determination of cyanide and thiocyanate in plasma by chemical ionization gas chromatography mass-spectrometry (CI-GC-MS). *Analytical and Bioanalytical Chemistry* 404, 2287-2294.

3. Logue, B.A., Kirschten, N.P., Petrikovics, I., Moser, M.A., Rockwood, G.A., Baskin, S.I., 2005. Determination of the cyanide metabolite 2-aminothiazoline-4-carboxylic acid in urine and plasma by gas chromatography-mass spectrometry. *J Chromatogr B: Analyt Technol Biomed Life Sci* 819, 237-44.

4. Bhandari, R. K., Oda, R. P., Petrikovics, I., Thompson, D., Mohan, S. B., Brenner, M., Rockwood, G. A., Logue, B. A. Cyanide Toxicokinetics: The Behavior of Cyanide, Thiocyanate and 2-amino-2-thiazoline-4-carboxylic Acid (ATCA) following Cyanide Exposure (Manuscript in preparation).

REFERENCES-Chapter 4

1. Sano, A., Takezawa, M., and Takitani, S., 1989 Spectrofluorometric determination of cyanide in blood and urine with naphthalene-2,3-dialdehyde and taurine. *Analyt Chim Acta* 225, 351-358.

2. Kosower, N. S. and Kosower, E. M., 1987. Thiol Llabeling with bromobimanes, *Meth. Enzymol* 143, 76-84.

3. Guidance for Industry Bioanalytical Method Validation 2001.

4. Bhandari, R. K., Manandhar, E., Oda, R. P., Rockwood, G. A., and Logue, B. A. 2013. Simultaneous high-performance liquid chromatography-tandem mass spectrometry (HPLC-MS-MS) analysis of cyanide and thiocyanate from plasma. (Manuscript in preparation).

REFRENCES-Chapter 5

1. Simeonova, F. P. Fishbein, L. 2004. Hydrogen cyanide and cyanides: human health aspects. *Concise Int Chem Assess Doc* 61, i-iv, 1-67.

2. Szinicz, L. 2005. History of chemical and biological warfare agents. *Toxicol* 214, 167-181.

3. Baskin, S. I. Brewer, T. 1997. *Textbook of Military Medicine, Medical Aspects of Chemical and Biological Warfare*; Borden Institute.

4. Lundquist, P. Rosling, H. Sorbo, B. Tibbling, L. 1987. Cyanide concentrations in blood after cigarette smoking, as determined by a sensitive fluorimetric method. *Clin Chem* 33, 1228-30.

5. Flora, S. J. S.; Romano, J. A.; Baskin, S. I.; Sekhar, K.; Eds: 2004. *Pharmacological Perspectives of Toxic Chemicals and Their Antidotes* Springer GmbH. .

6. Norris, J. C. Utley, W. A. Hume, A. S. 1990. Mechanism of antagonizing cyanide-induced lethality by α-ketoglutaric acid. *Toxicol* 62, 275-83.

7. Wagner, B. M. Donnarumma, F. Wintersteiger, R. Windischhofer, W. Leis, H. J. 2010. Simultaneous quantitative determination of α-ketoglutaric acid and 5-hydroxymethylfurfural in human plasma by gas chromatography-mass spectrometry. *Anal Bioanal Chem* 396, 2629-2637.

8. Bebarta, V. S. Tanen, D. A. Lairet, J. Dixon, P. S. Valtier, S. Bush, A., 2010. Hydroxocobalamin and sodium thiosulfate versus sodium nitrite and sodium thiosulfate in the treatment of acute cyanide toxicity in a swine (Sus scrofa) model. *Annals of Emergency Medicine* 55 (4), 345-51.

9. Mitchell BL, Rockwood GA, Logue BA. 2013. Quantification of cyanide metabolite α-ketoglutarate cyanohydrin in plasma by ultra high-performance liquid chromatography tandem mass spectrometry. *J. Chromatogr. B* (Manuscript accepted).

10. Mitchell B.L., Bhandari R.K., Bebarta V.S., Rockwood G.A., Boss G.R., and Logue B.A. 2013 Toxicokinetic profiles of α-ketoglutarate cyanohydrin, a cyanide detoxification product, following exposure to potassium cyanide. *Toxicology Letters* (Manuscript accepted).

REFERENCES-Chapter 6

1. Meister, A. and Anderson, M. E., 1983 Glutathione. *Ann Rev Biochem* 52, 711-760.

2. Jose, C. J., Jacob, R. H., Gardner, G. E., Pethick, D. W., and Liu, S. M., 2010. Selenium supplementation and increased muscle glutathione concentration do not improve the color stability of lamb meat. *J Agric Food Sci* 58 (12), 7389-7393.

3. Serru, V., Baudin, B., Ziegler, F., David, J-P., Cals, M-J., Vaubourdolle, M., and Mario, N., 2001. Quantification of reduced and oxidized glutathione in whole blood samples by capillary electrophoresis. *Clin Chem 47* (7), 1321-1324.

4. Michelet, F., Gueguen, R., Leroy, P., Wellman, M., Nicolas, A., and Siest, G., 1995. Blood and plasma glutathione measured in healthy subjects by HPLC: Relation to sex, aging, biological variables, and life habits. *Clin Chem* 41 (10), 1509-1517.

5. Hatch, R. C., Laflamme, D. P., and Jain, A. V., 1990. Effects of various known and potential cyanide antagonists and a glutathione depletor on acute toxicity of cyanide in mice. *Vet Human Toxicol* 32 (1), 9-16.

6. Catsimpoolas, N., and Wood, J. L., 1964. The reaction of cyanide with bovine serum albumin. *J Biol Chem* 239 (12), 4132-4137.

7. Youso, S. L., Rockwood, G. A., Lee, J. P., Logue, B. A., 2010. Determination of cyanide exposure by gas chromatography-mass spectrometry analysis of cyanide-exposed plasma proteins. *Anal Chim Acta* 677 (1), 24-28.

8. Nagasawa, H. T., Cummings, S. E., and Baskin, S. I., 2004. The structure of "ITCA", a urinary metabolite of cyanide. *Organic Prep and Proc Int'l* 36 (2), 178-182.

9. Ellman, G. L., 1959. Tissue sulfhydryl groups. *Arch Biochem Biophys* 82, 70-77.

10. Habeeb, A. F. S. A., 1972. Reaction of protein sulfhydryl groups with Ellman's reagent. *Methods Enzymol. 25 (part B)* 457-464.

REFERENCES-Chapter 7

1. Petrikovics I, Kuzmitcheva G, Budai M, Haines D, Nagy A, Rockwood GA, Way JL. 2010. Encapsulated rhodanese with two new sulfur donors in cyanide antagonism. In *XII International Congress of Toxicology* Barcelona, Spain.

2. Frankenberg L. 1980. Enzyme therapy in cyanide poisoning: effect of rhodanese and sulfur compounds. *ArchToxicol* 45, 315-323.

3. Iciek M, Wlodek L 2001 Biosynthesis and biological properties of compounds containing highly reactive, reduced sulfane sulfur. *Pol J Pharmacol* 53, 215-225.

4 Petrikovics I, Pei L, McGuinn W, Cannon E, Way J. 1994. Encapsulation of rhodanese and organic thiosulfonates by mouse erythrocytes. *Fund and Appl Toxicol* 23, 70-75.